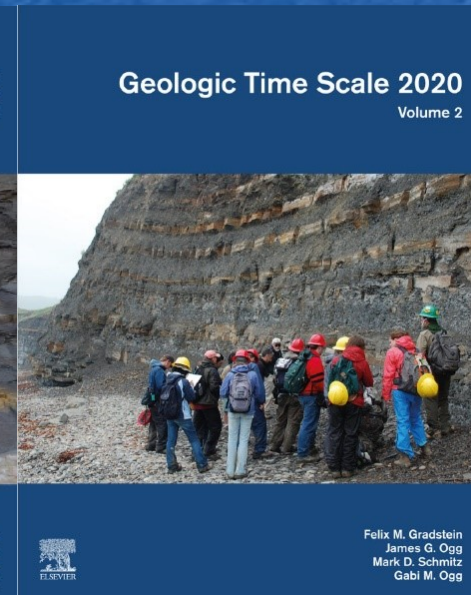
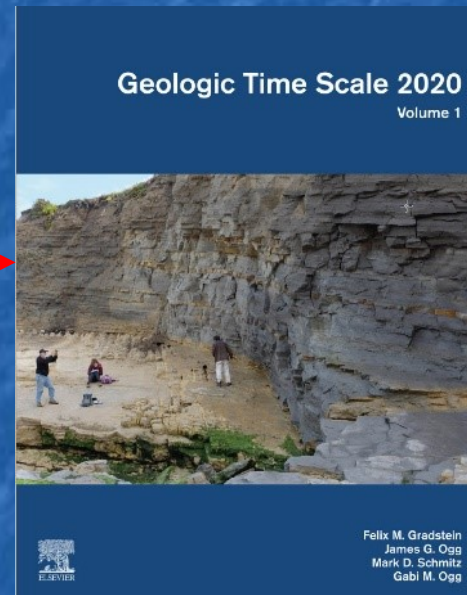
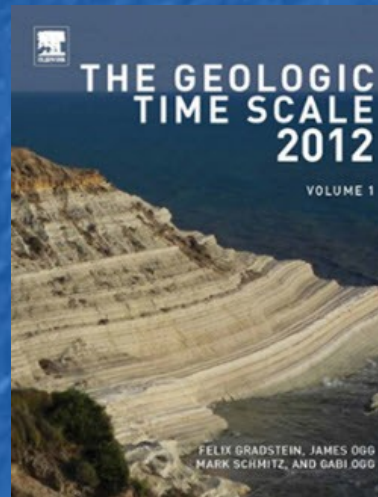
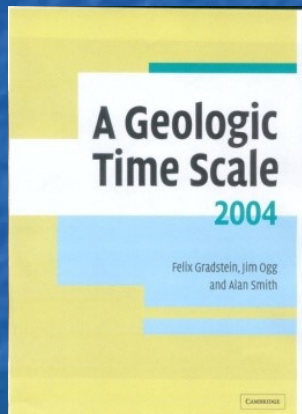
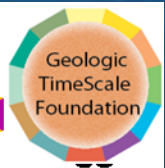


Geologic Time Scale 2020, with special reference to the Cretaceous Period.

Felix M. Gradstein



<http://www.tscreator.com>



Cenozoic	Neogene	Pliocene	
		Miocene	
		Paleogene	
		Oligocene	
Mesozoic	Cretaceous	Late	
		Early	
	Jurassic	Late	
		Middle	
		Early	
	Triassic	Late	
		Middle	
		Early	
	Paleozoic	Permian	Lopingian
			Guadalupian
Cisuralian			
Carboniferous		Pinites-lymanian	Late
			Early
		Mississippian	Late
			Middle
			Early
Devonian	Late		
	Middle		
	Early		
Silurian	Pragian		
	Ludlow		
	Wenlock		
Ordovician	Llandovery		
	Late		
	Early		
Cambrian	Furongian		
	Middle		
	Early		

Why a new Geologic Time Scale ?

- Better built, more accurate and more precise
- 75 of 103 stage boundaries formally defined versus < 60 in 2012
- Cenozoic orbitally tuned (20 - 40 kyr accuracy); some cycle scaling of Cretaceous, Jurassic, lower Triassic and Carboniferous stages
- 330 U/Pb and Ar/Ar ages (> 125 new since GTS2012) a majority < 0.5 myr external uncertainty
- Improved statistical interpolations with detailed error analysis
- > 30 Phanerozoic stage boundaries changed age 0.5 - 6 Ma
- Sixteen more chapters (now 45), including Phanerozoic Eustasy, Chemostratigraphy, Evolution/Biostratigraphy, Crustal Events

The Geologic Time Scale 2020

Volume 1

Chapter 1, Introduction

Chapter 2, The Chronostratigraphic Scale

Chapter 3, Evolution and Biostratigraphy

Chapter 3A, Trilobites

Chapter 3B, Graptolites

Chapter 3C, Chitinozoans

Chapter 3D, Conodonts

Chapter 3E, Ammonoidea

Chapter 3F, Calcareous nannofossils

Chapter 3G, Planktonic foraminifera

Chapter 3H, Larger foraminifera

Chapter 3I, Dinoflagellates

Chapter 3J, Plants, spores and pollen

Chapter 3K, Microcrinoids

Chapter 3L, Three major mass extinctions
and Evolutionary Radiations in their Aftermath

Chapter 4, Astrochronology

Chapter 5, Magnetostratigraphy

Chapter 6, Radiogenic isotopes geochronology

Chapter 7, Strontium isotope stratigraphy

Chapter 8, Osmium isotope stratigraphy

Chapter 9, Sulphur isotope stratigraphy

Chapter 10, Oxygen isotope stratigraphy

Chapter 11, Carbon isotope stratigraphy

Chapter 12, Crustal events

Chapter 12A, Influence of LIP's

Chapter 12B, Paleogeographic reconstructions

Chapter 13, Phanerozoic eustasy

Chapter 14A, Geomathematical and statistical procedures

Chapter 14B, Global composite sections and constrained
optimization

Volume 2

Chapter 15, The Planetary Time Scale

Chapter 16, The Precambrian

Chapter 17, The Tonian and Cryogenian Periods

Chapter 18, The Ediacaran Period

Chapter 19, The Cambrian Period

Chapter 20, The Ordovician Period

Chapter 21, The Silurian Period

Chapter 22, The Devonian Period

Chapter 23, The Carboniferous Period

Chapter 24, The Permian Period

Chapter 25, The Triassic Period

Chapter 26, The Jurassic Period

Chapter 27, The Cretaceous Period

Chapter 28, The Paleogene Period

Chapter 29, The Neogene Period

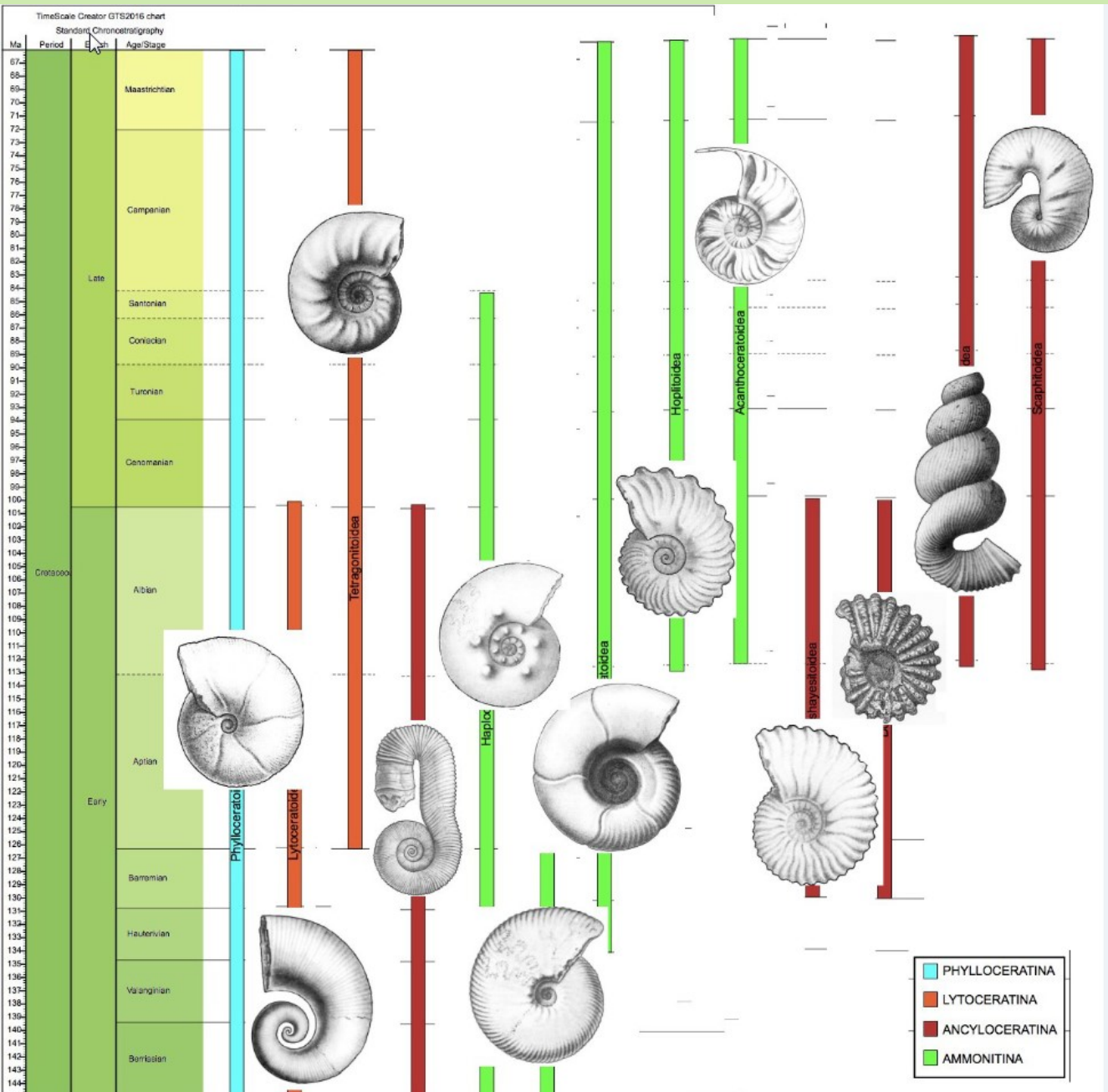
Chapter 30, The Quaternary Period

Chapter 31, The Anthropocene 'Period'

Appendix 1, Recommended color coding of stages

Appendix 2, Radiometric ages used in GTS2020

Principal Cretaceous ammonite genera



Subchapter 3E

Ammonoidea

A.S. Gale, D. Korn, A.J. McGowan, J. Cope and C. Ifrim



Andy Gale

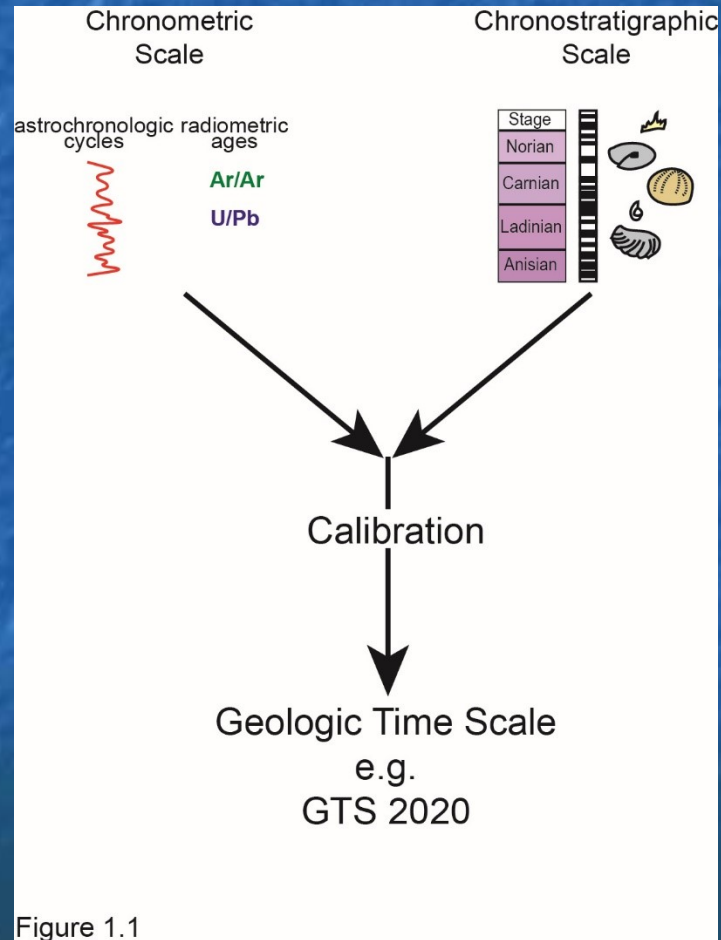
The Time Scale Components

The stratigraphic divisions and their correlation in the rocks

Measuring linear time or elapsed durations from the rocks

The methods of joining the stratigraphic and the linear scales

Jurassic	Late	Tithonian	
		Kimmeridgian	
		Oxfordian	
	Middle	Callovian	
		Bathonian	
		Bajocian	
		Aalenian	
	Early	Toarcian	
		Pliensbachian	
Sinemurian			
Hettangian			
Triassic	Late	Rhaetian	
		Norian	
		Carnian	
	Middle	Ladinian	
		Anisian	
	Early	Olenekian	
		Induan	
	Permian	Lopingian	Changhsingian Wuchiapingian
		Guadalupian	Capitanian
Wordian			
Roadian			
Cisuralian		Kungurian	
		Artinskian	
		Sakmarian	
		Asselian	
		Gzhelian	
	Kasimovian		
Carboniferous	Pennsylvanian	Late	Kasimovian
		Middle	Moscovian
		Early	Bashkirian
	Mississippian	Late	Serpukhovian
		Middle	Visean
			Tournaisian
		Early	Tournaisian

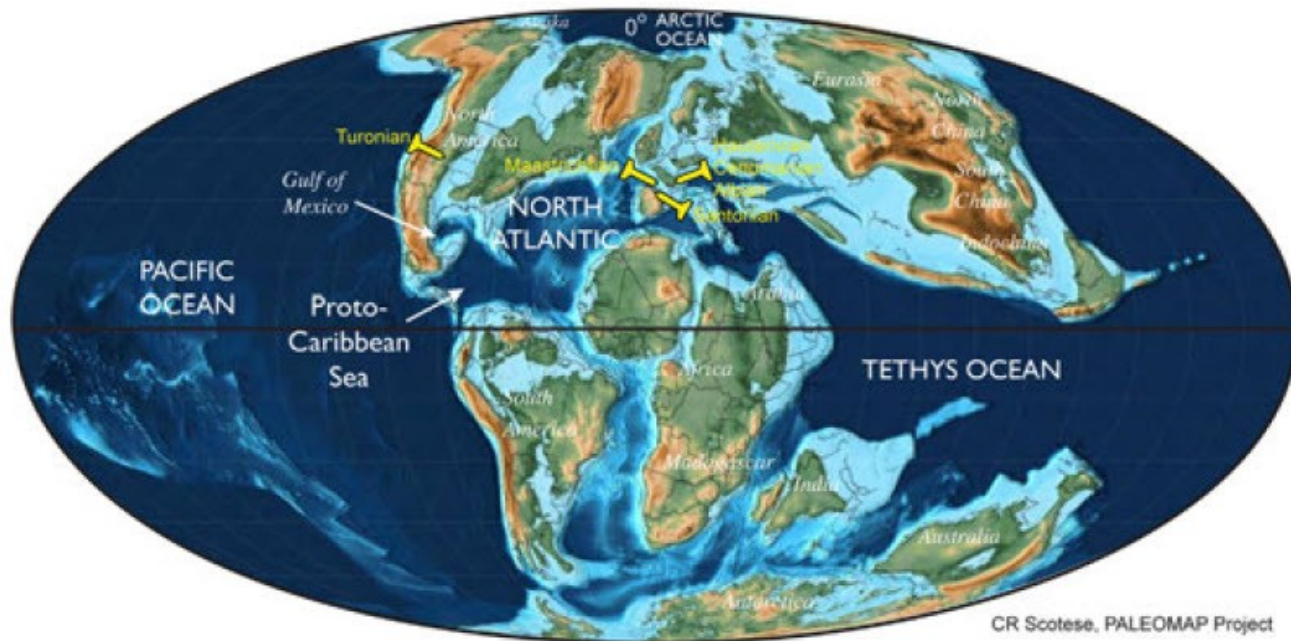


Jurassic	Upper	Tithonian	
		Kimmeridgian	
		Oxfordian	
	Middle	Callovian	
		Bathonian	
		Bajocian	
		Aalenian	
	Lower	Toarcian	
		Pliensbachian	
Sinemurian			
Hettangian			
Triassic	Upper	Rhaetian	
		Norian	
		Carnian	
	Middle	Ladinian	
		Anisian	
	Lower	Olenekian	
		Induan	
	Permian	Lopingian	Changhsingian Wuchiapingian
		Guadalupian	Capitanian
Wordian			
Roadian			
Cisuralian		Kungurian	
		Artinskian	
		Sakmarian	
		Asselian	
		Gzhelian	
	Kasimovian		
Carboniferous	Pennsylvanian	Upper	Kasimovian
		Middle	Moscovian
		Lower	Bashkirian
	Mississippian	Upper	Serpukhovian
		Middle	Visean
			Tournaisian
		Lower	Tournaisian

Figure 1.1

The Cretaceous Period

96.6 Ma Cretaceous

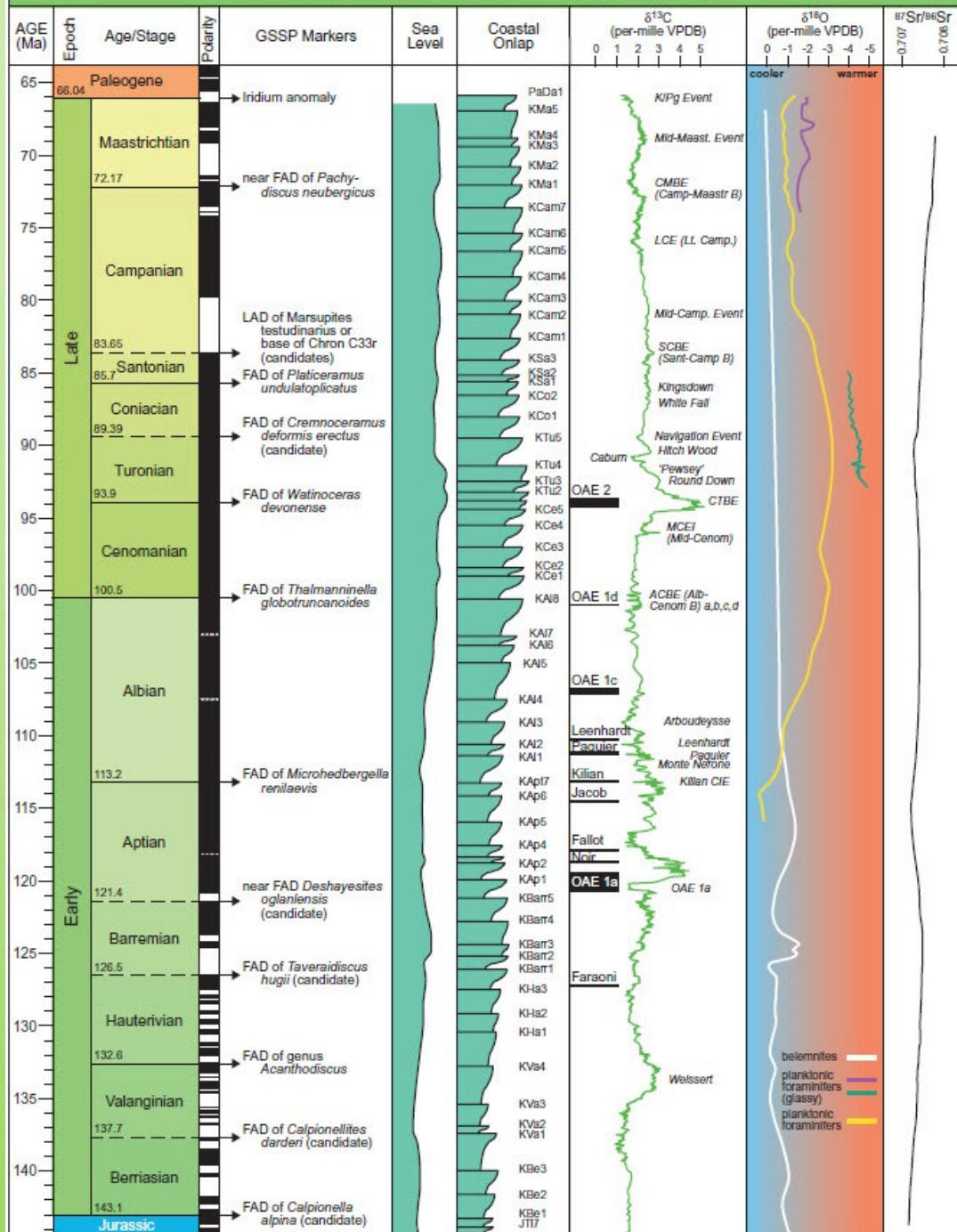


Tethys time – global super Ocean



Andy Gale

Cretaceous Time Scale



Boundaries of the twelve historical Cretaceous stages primarily defined by ammonites in France and The Netherlands.

Magnostratigraphy, microfossil zones or events and carbon isotope excursions added later.

Six ratified and six potential Global Boundary Sections and Points (GSSP's)

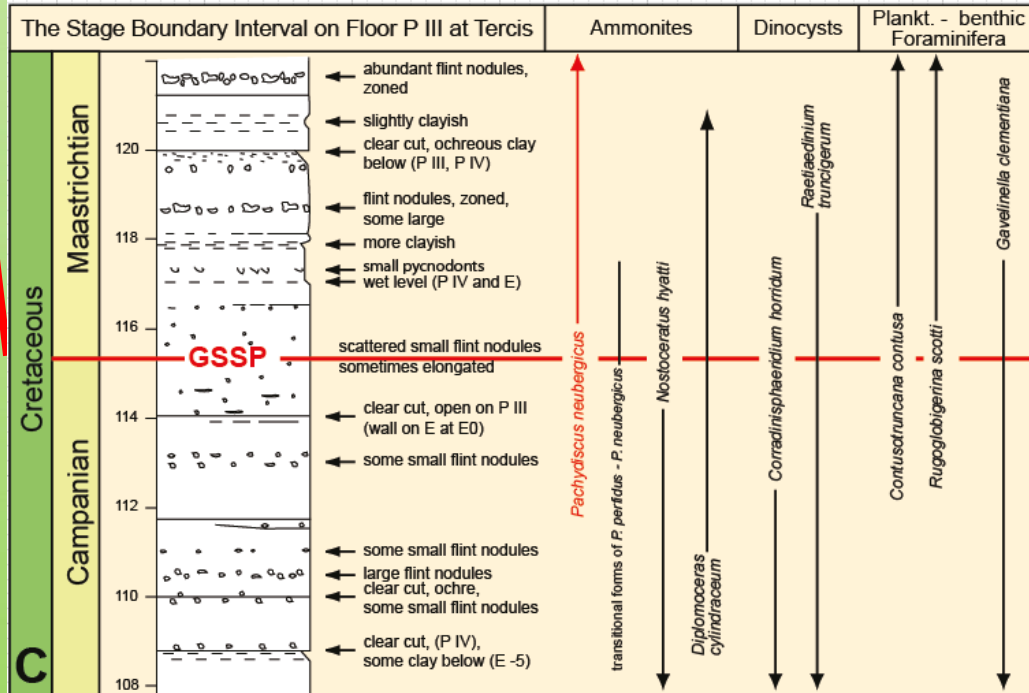
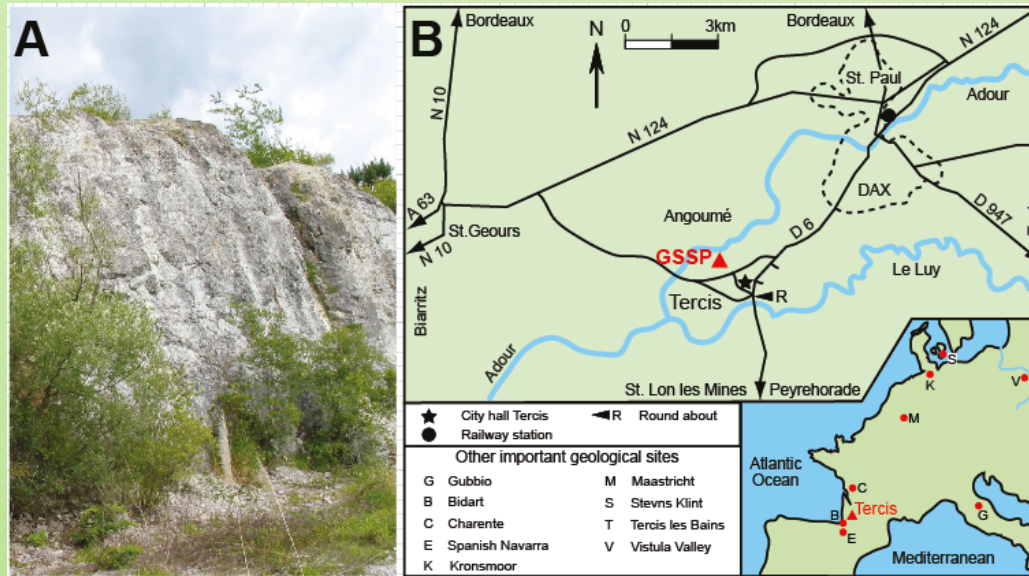
GSSPs of the Cretaceous Stages, with location and primary correlation criteria

Stage	GSSP Location	Latitude, Longitude	Boundary Level	Correlation Events	Reference
Maastrichtian	Tercis les Bains, Landes, France	43°40'46.1"N 1°06'47.9"W*	level 115.2 on platform IV of the geological site at Tercis les Bains	Mean of 12 biostratigraphic criteria of equal importance. Near ammonite FAD of <i>Pachydiscus neubergicus</i>	Episodes 24/4, 2001
<i>Campanian</i>	<i>candidates are in Italy and in Texas</i>			<i>Crinoid, LAD of Marsupites testudinarius or base of Chron C33r</i>	
Santonian	Olazagutia, Northern Spain	42°52'5.3"N 2°11'40"W	94.4 m in the eastern border of the Cantera de Margas quarry	Inoceramid bivalve, FAD <i>Platyceramus undulatopectatus</i>	Episodes 37/1, 2014
<i>Coniacian</i>	<i>candidates are in Poland (Slupia Nadbrzena) and Germany (Salzgitter)</i>			<i>Inoceramid bivalve, FAD of Cremnoceramus deformis erectus</i>	
Turonian	Pueblo, Colorado, USA	38°16'56"N 104°43'39"W*	base of Bed 86 of the Bridge Creek Limestone Member	Ammonite, FAD of <i>Watinoceras devonense</i>	Episodes 28/2, 2005
Cenomanian	Mont Risou, Hautes-Alpes, France	44°23'33"N 5°30'43"E	36 m below the top of the Marnes Bleues Formation on the south side of Mont Risou	Foraminifer, FAD of <i>Thalmaninella globotruncanoides</i>	Episodes 27/1, 2004
Albian	Col de Pré-Guittard Section, Drôme, France	44°29'47"N 5°18'41"E	37.4 m above the base of the Marnes Bleues Formation and 40 cm above the base of the Kilian Niveau	Foraminifer, FAD of <i>Microhedbergella renilaevis</i>	Episodes 40/3, 2017
<i>Aptian</i>	<i>candidate is Gorgo a Cerbara, Umbria-Marche, central Italy</i>			<i>Base of Chron M0r; near ammonite, FAD of Deshayesites oglanlensis</i>	
<i>Barremian</i>	<i>candidate is Rio Argos near Caravaca, Murcia province, Spain</i>			<i>Ammonite, FAD of Taveraidiscus hugii</i>	
Hauterivian	La Charce Section, Drôme Province, southeast France	44°28'10"N 5°26'37.4"E	base of Bed 189 of La Charce Section	Ammonite, FAD of genus <i>Acanthodiscus</i>	
<i>Valanginian</i>	<i>candidate is near Caravaca (S. Spain)</i>			<i>Calpionellid, FAD of Calpionellites darderi</i>	
<i>Berriasian</i>	<i>Tré Maroua, SE of Gap, southeast France</i>			<i>Calpionellid, FAD of Calpionella alpina</i>	

* a

GSSP for the Maastrichtian Stage

Upper	Maastrichtian
	Campanian
	Santonian
	Coniacian
	Turonian
	Cenomanian
Lower	Albian
	Aptian
	Barremian
	Hauterivian
	Valanginian
	Berriasian



GSSP for base of Maastrichtian Stage at Tercis, France is **90-cm below** lowest occurrences of ammonoids *Pachydiscus neubergicus* and *Hoploscaphites constrictus*.

Difficult GSSP in the Tercis section, France

No real GSSP, no geomagnetics and no good planktonic events

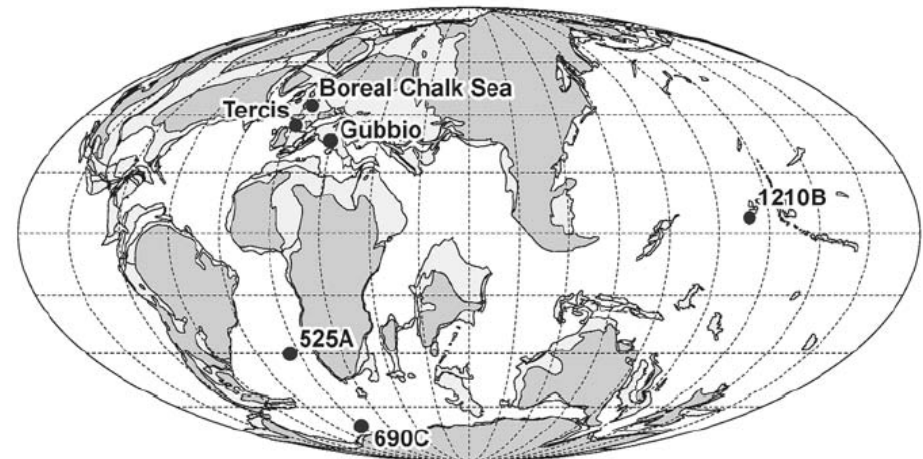


Newsletters on Stratigraphy, Vol. 45/1, 25–53
Stuttgart, April 2012

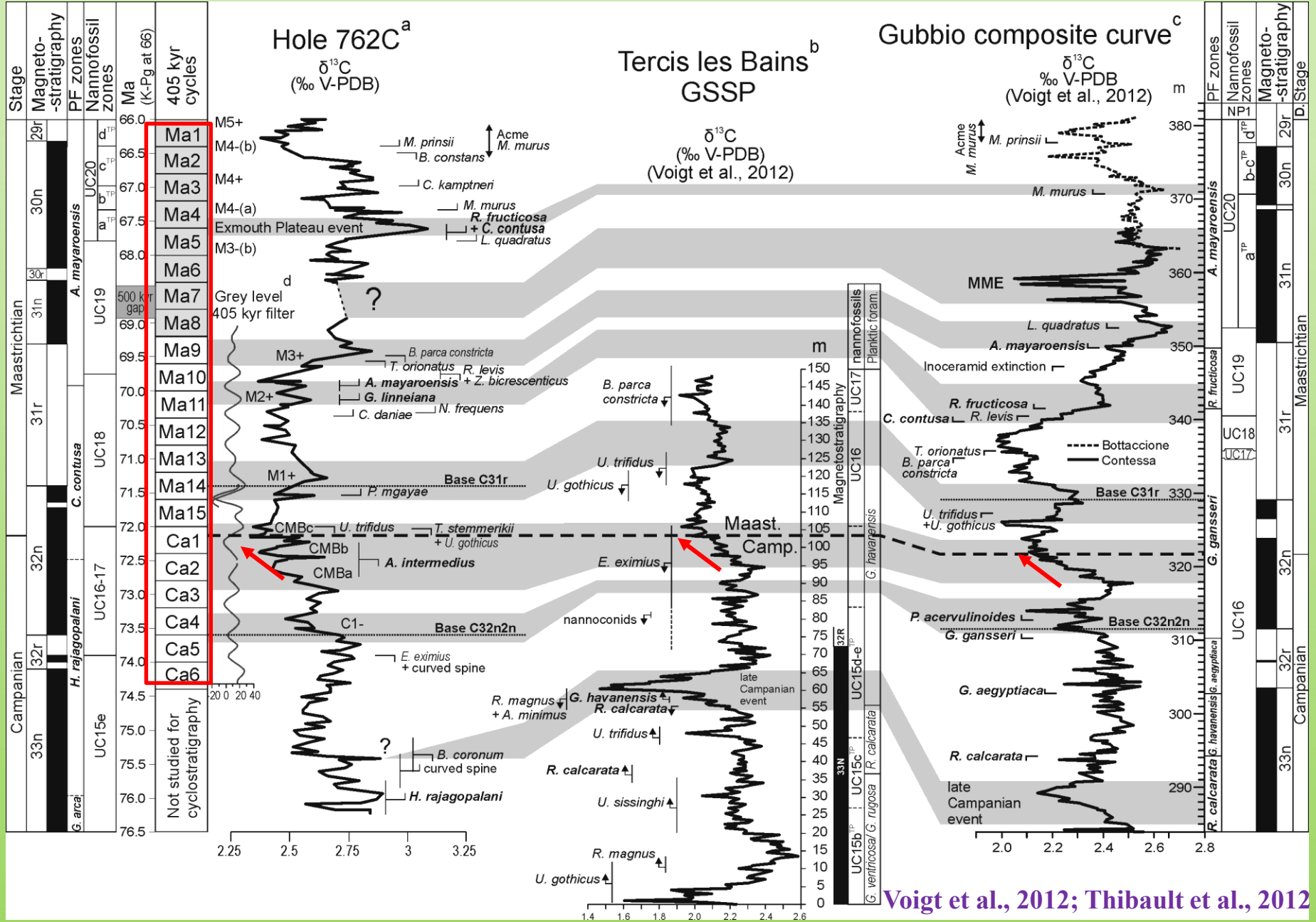
Article

Global correlation of Upper Campanian – Maastrichtian successions using carbon-isotope stratigraphy: development of a new Maastrichtian timescale

Silke Voigt¹, Andrew S. Gale², Claudia Jung¹, and Hugh C. Jenkyns³

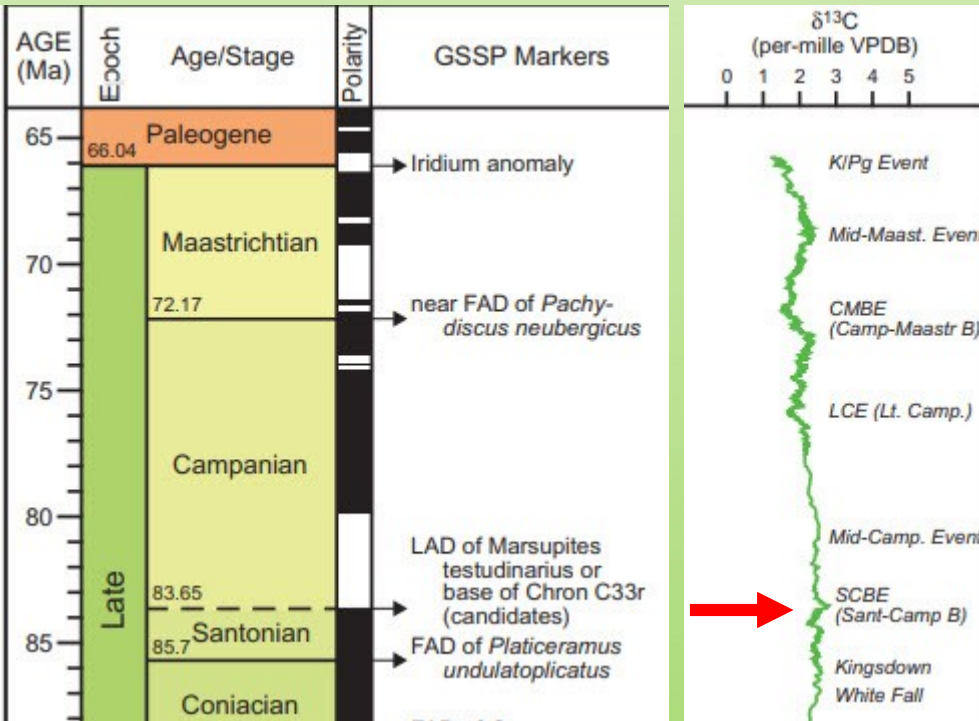


Inter-basinal correlations and 405 kyr cycles



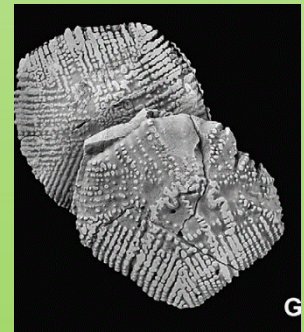
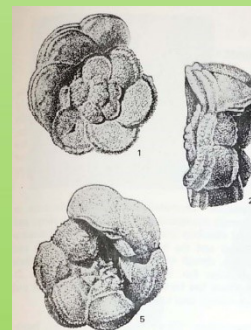
Santonian-Campanian boundary

Two separate bug definitions have grown up on account of provinciality and usage, solved by carbon isotopes that link crinoid and planktonic forams sections.

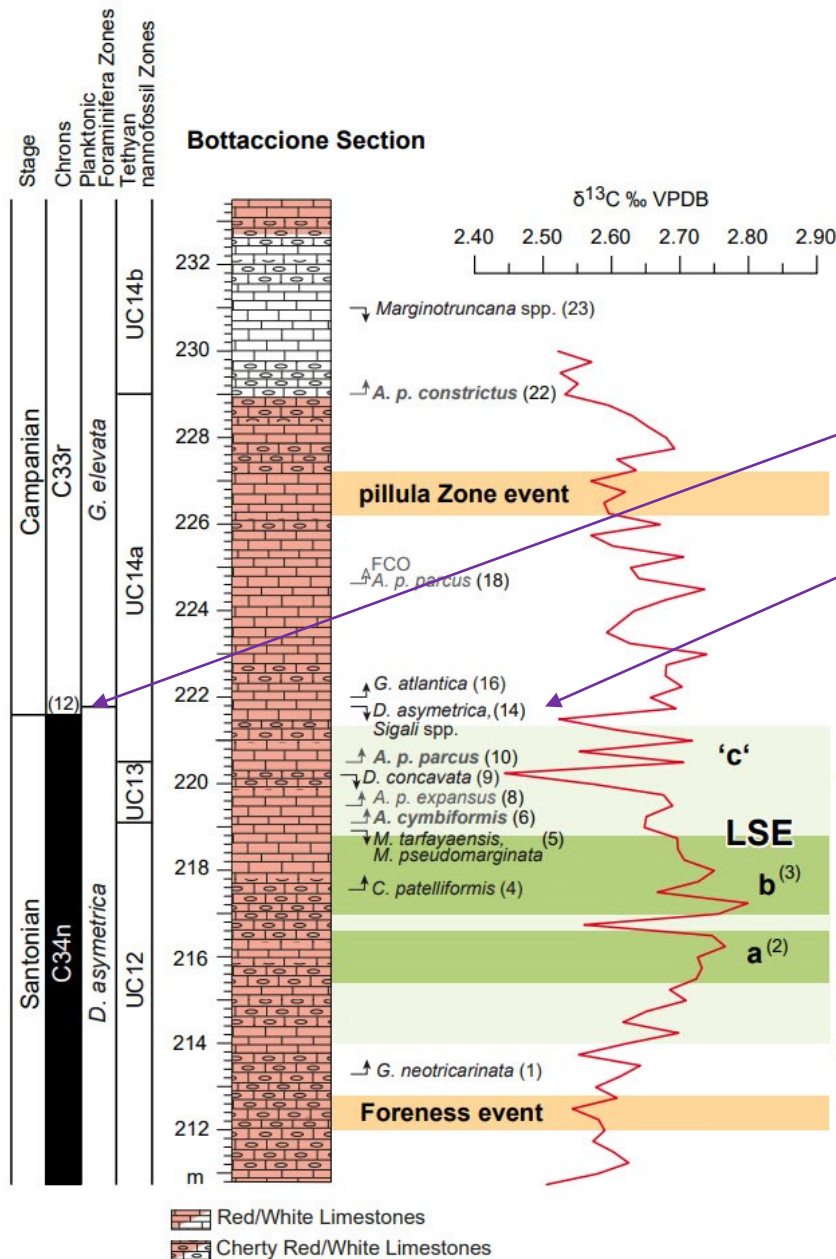


1. Use of crinoid *Marsupites* extinction in Boreal, Austral and some Tethyan regions, dominantly in chalks.

2 – Extinction of planktonic foram *D. asymmetrica* in relation to base of magnetochron 33R.



Proposed GSSP for the Santonian-Campanian boundary, Gubbio, Italy with magnetostratigraphy, carbon isotopes and biostratigraphy



Bottaccione Gorge at Gubbio, Umbria, Italy.

The beginning of Chron C33r, with global recognition in pelagic and continental settings.

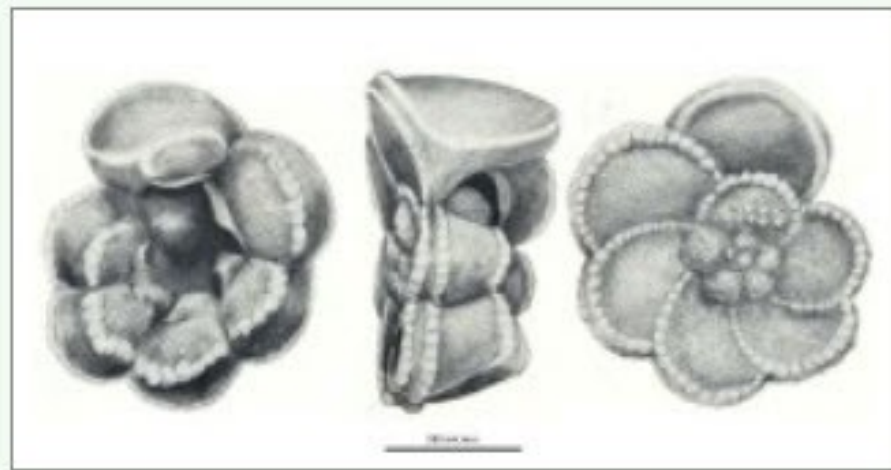
Close to the **extinction** of *D. asymetrica* and changes in the nannofossil *Broinsonia*.

Distinctive double (a, b) positive excursion in $\delta^{13}\text{C}$, (LSE – Late Santonian Event) enables detailed global correlation.



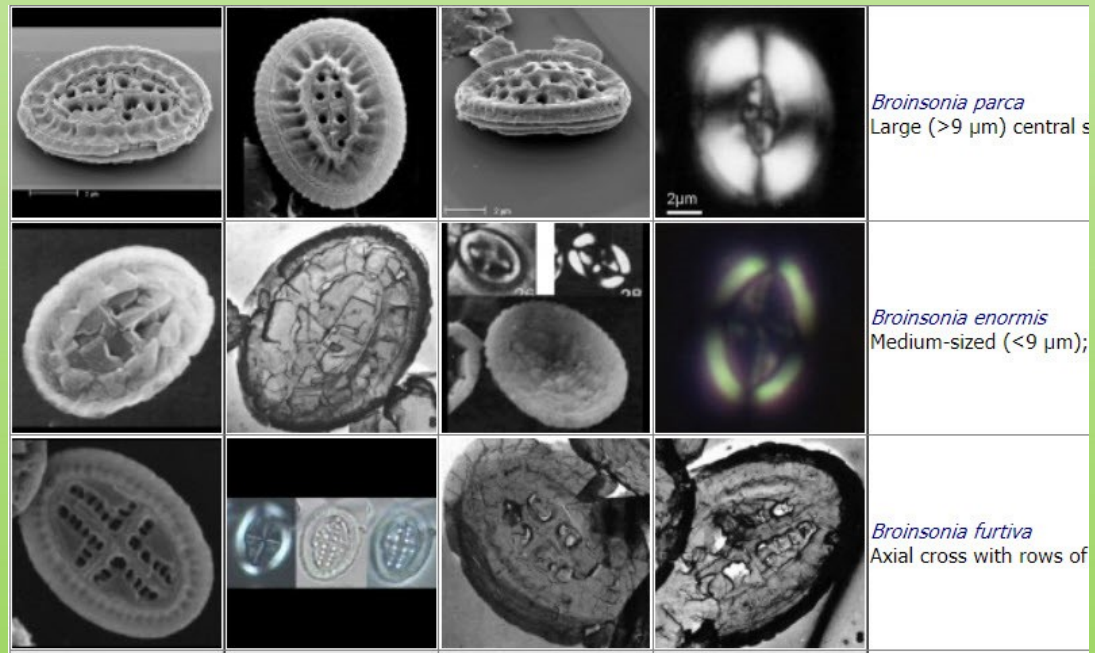
Principal Santonian-Campanian boundary markers

Dicarinella symmetrica (D. carinata) LAD

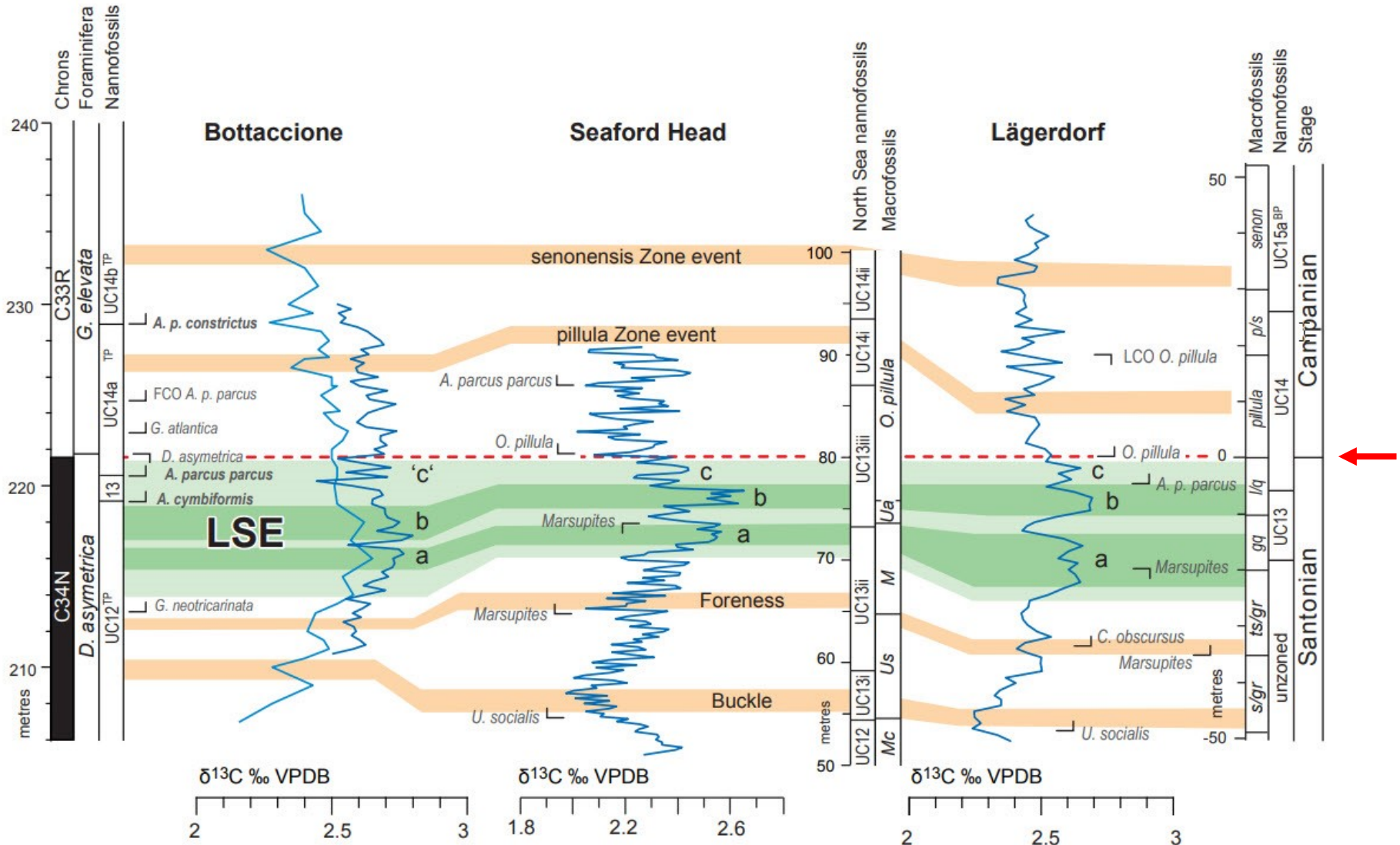


Postuma 1971 p025-4.JPG

Broinsonia parca var.

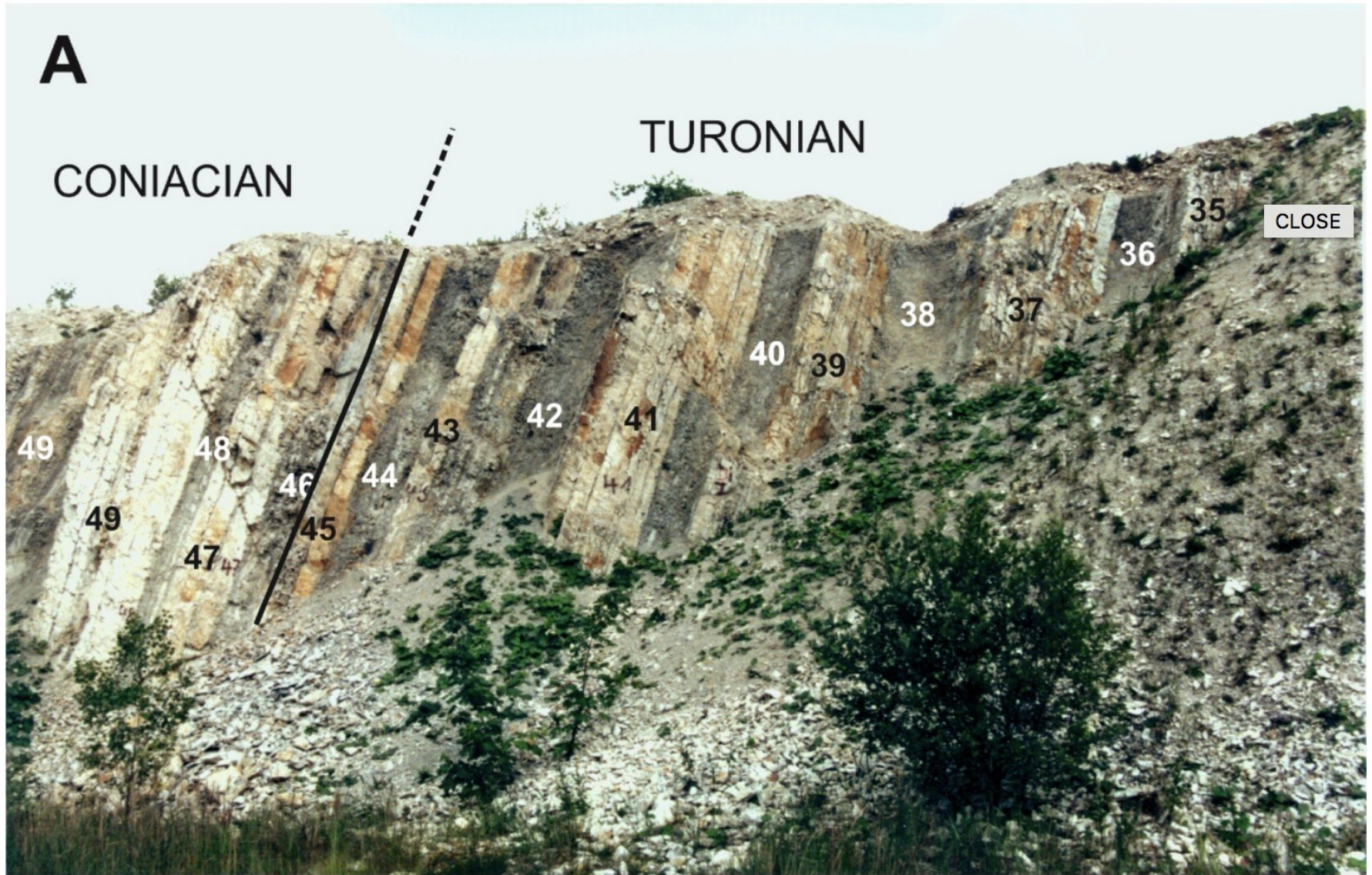


Correlation from Gubbio using carbon isotopes and biostratigraphy for Santonian-Campanian boundary correlation

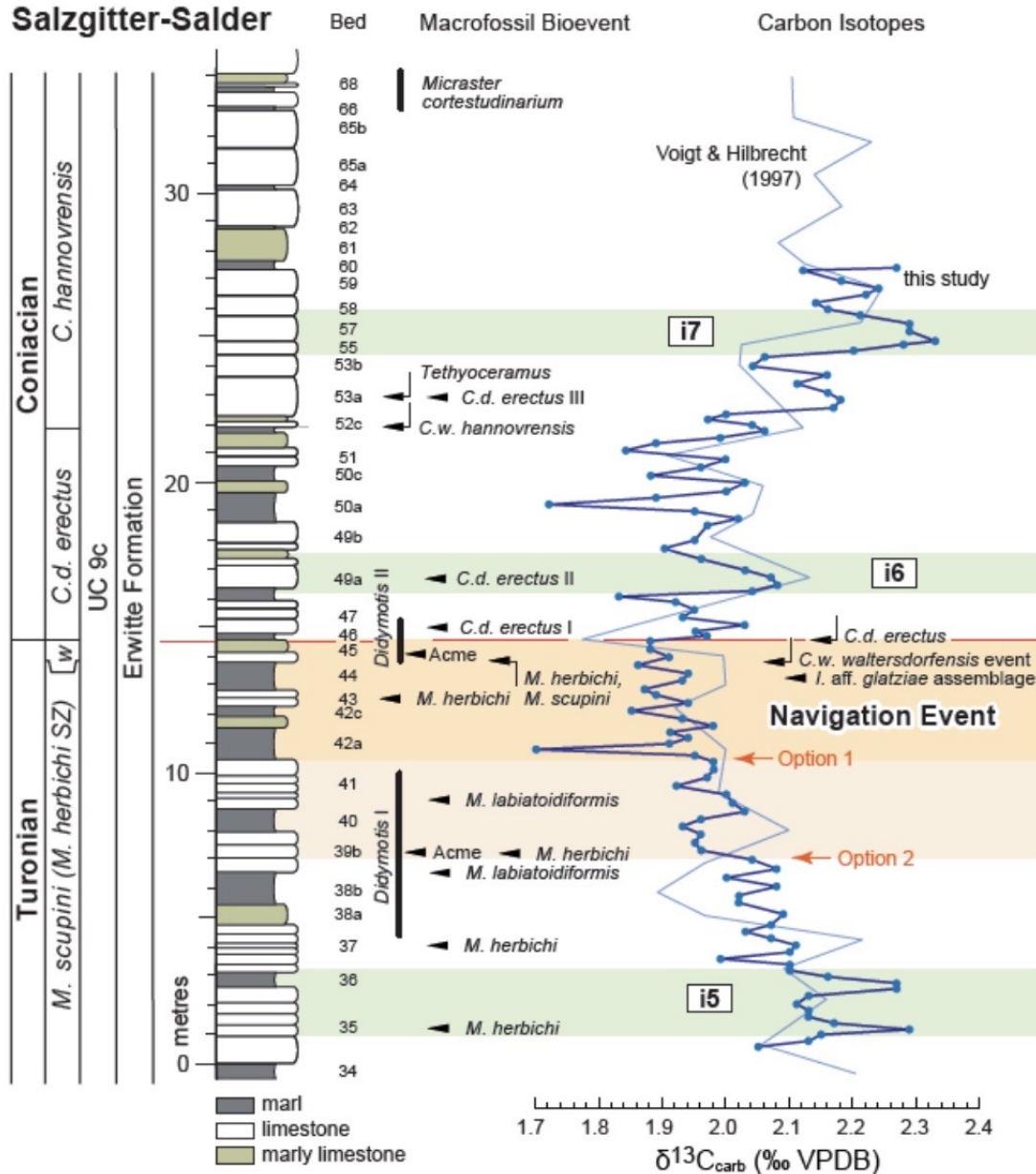


GSSP proposal for the Coniacian Stage

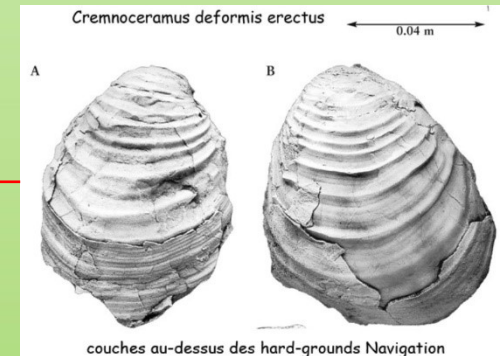
Salzgitter-Salder Quarry section (Lower Saxony, Germany)



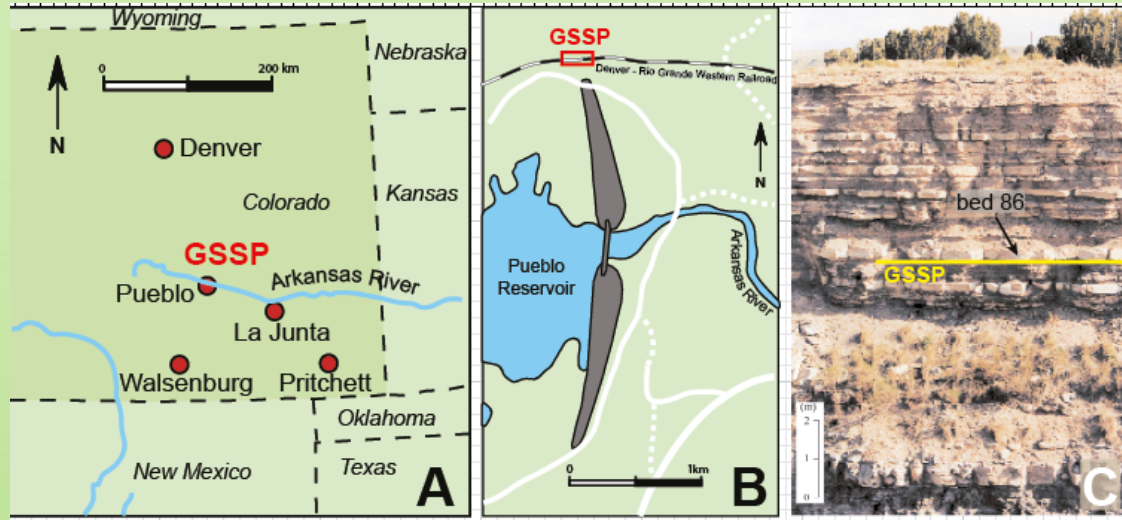
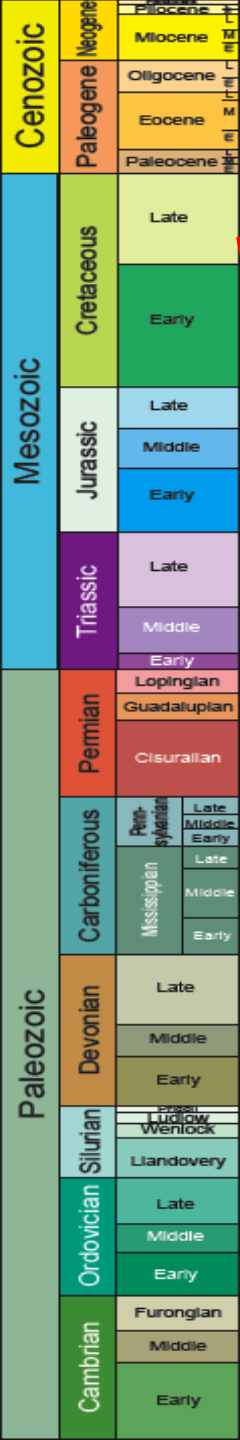
GSSP proposal Coniacian Stage



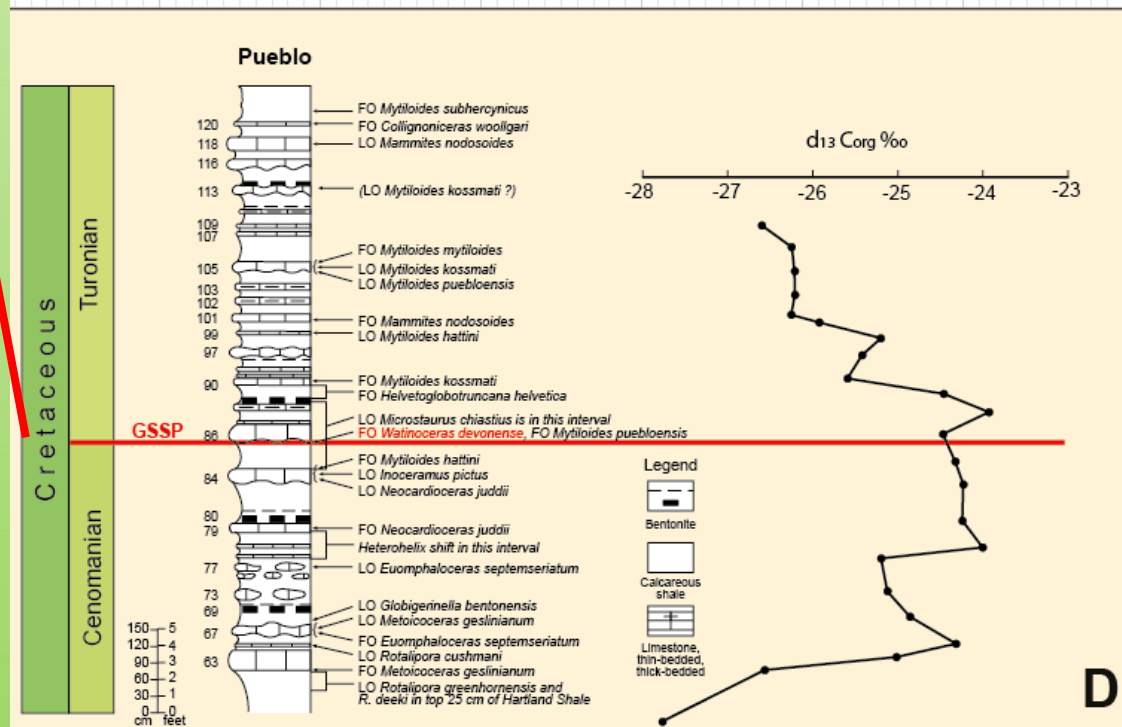
Salzgitter-Salder Quarry section
(Lower Saxony, Germany)



GSSP Turonian Stage



GSSP for base of the Turonian Stage near Pueblo, Colorado, USA. The GSSP level is LO *Watinoceras devonense*.

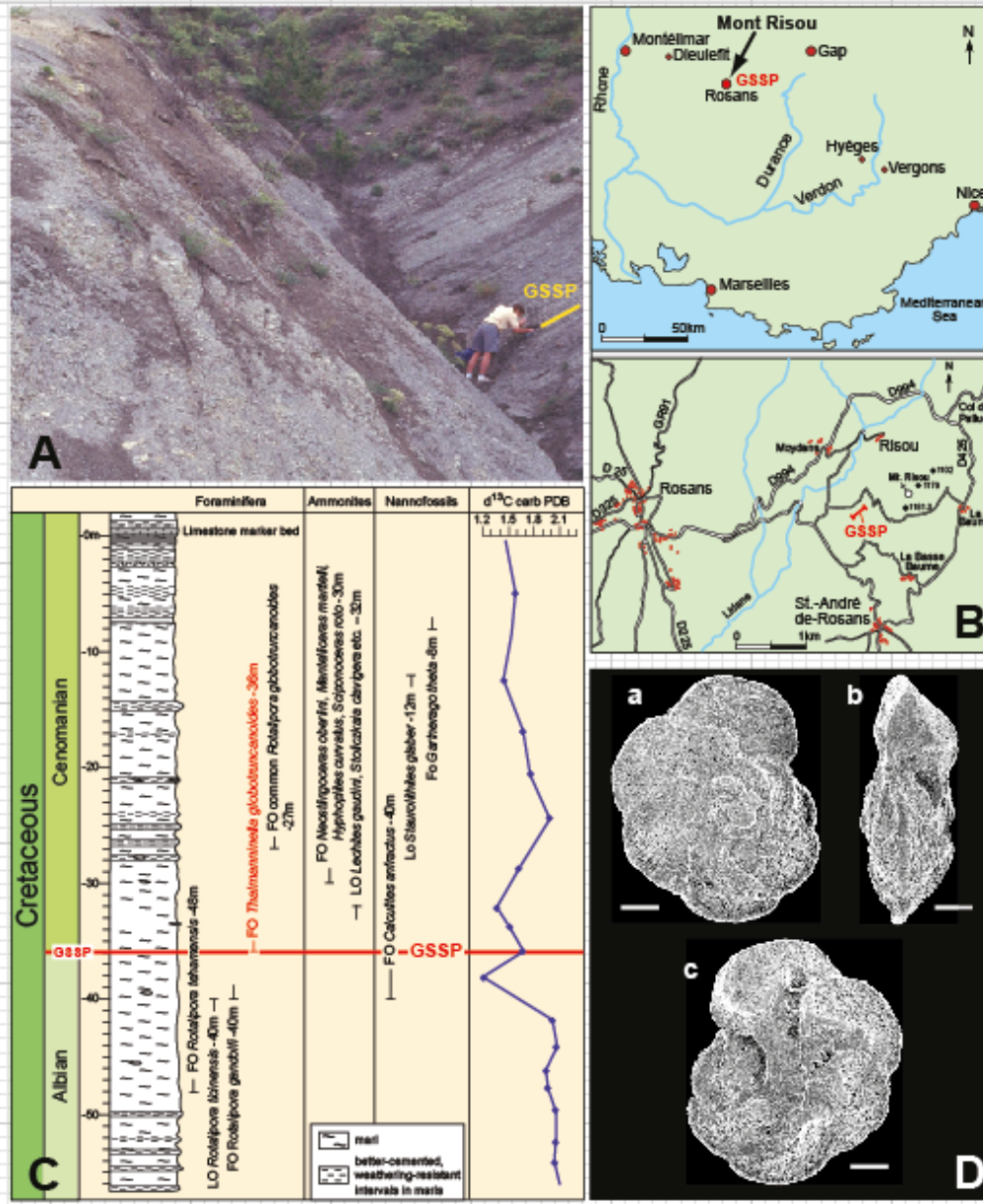


New high-precision age date 93.90 ± 0.15 (Meyers et al. 2012)

GSSP Cenomanian Stage

Cenozoic	Neogene	Pliocene	
	Paleogene	Oligocene	
		Eocene	
		Paleocene	
Mesozoic	Cretaceous	Late	
		Early	
	Jurassic	Late	
		Middle	
		Early	
	Triassic	Late	
		Middle	
		Early	
	Paleozoic	Permian	Guadalupian
			Cisuralian
Carboniferous		Petro-sylvanian	Late
			Early
		Mississippian	Late
			Middle
			Early
Devonian		Late	
		Middle	
		Early	
Silurian	Pragian		
	Llandovery		
	Wenlock		
	Llandovery		
Ordovician	Late		
	Middle		
	Early		
Cambrian	Furongian		
	Middle		
	Early		

Base of the Cenomanian Stage of the Cretaceous System, Mont Risou, Hautes-Alpes, France.



Boundary age of 100.5 ± 0.14 Ma.

Global correlation of Cenomanian sequences: Evidence for Milankowitch control on sea level

Gale et al., 2002, GSA Bulletin.

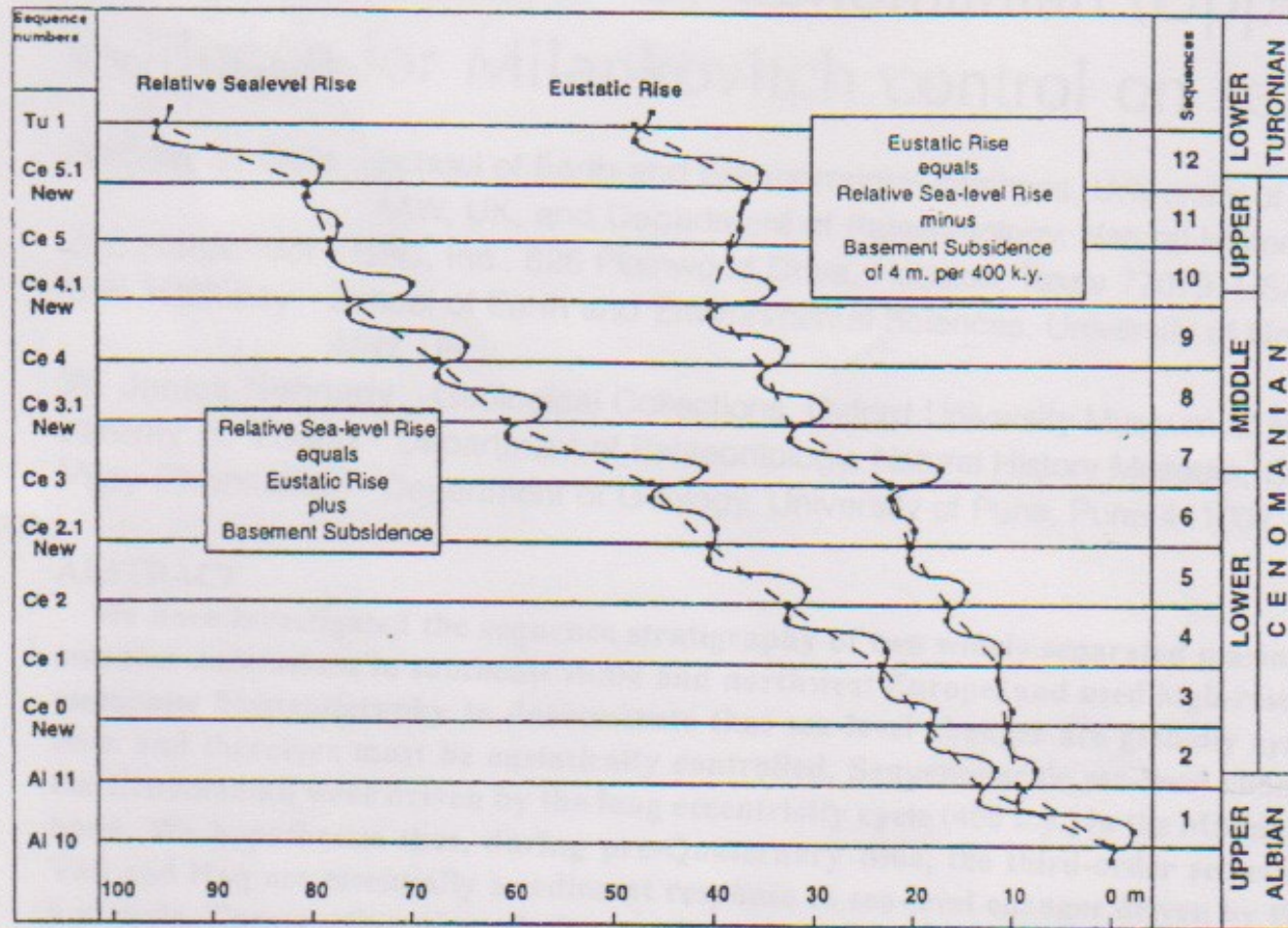


Figure 4. Comparison of relative sea-level rise with eustatic rise for Odiyam-Kunnam region in Cauvery Basin, estimating basement thermal contraction subsidence as 4 m/400 k.y. Short-term sea-level changes for 12 sequences, measured from incised valleys, are superimposed on long-term relative sea-level rise and eustatic rise.



Andy Gale



Jan Hardenbol

The Carbon Isotope Curve

$$\delta^{13}\text{C} = \frac{\{(^{13}\text{C}/^{12}\text{C}) \text{ sample} - (^{13}\text{C}/^{12}\text{C}) \text{ standard}\} \times 1000}{(^{13}\text{C}/^{12}\text{C}) \text{ standard}}$$

Stratigraphically powerful curve of changes in $^{12}\text{C}/^{13}\text{C}$ ratio of dissolved carbon in the ocean/atmosphere system
measured for example in foraminiferal shells

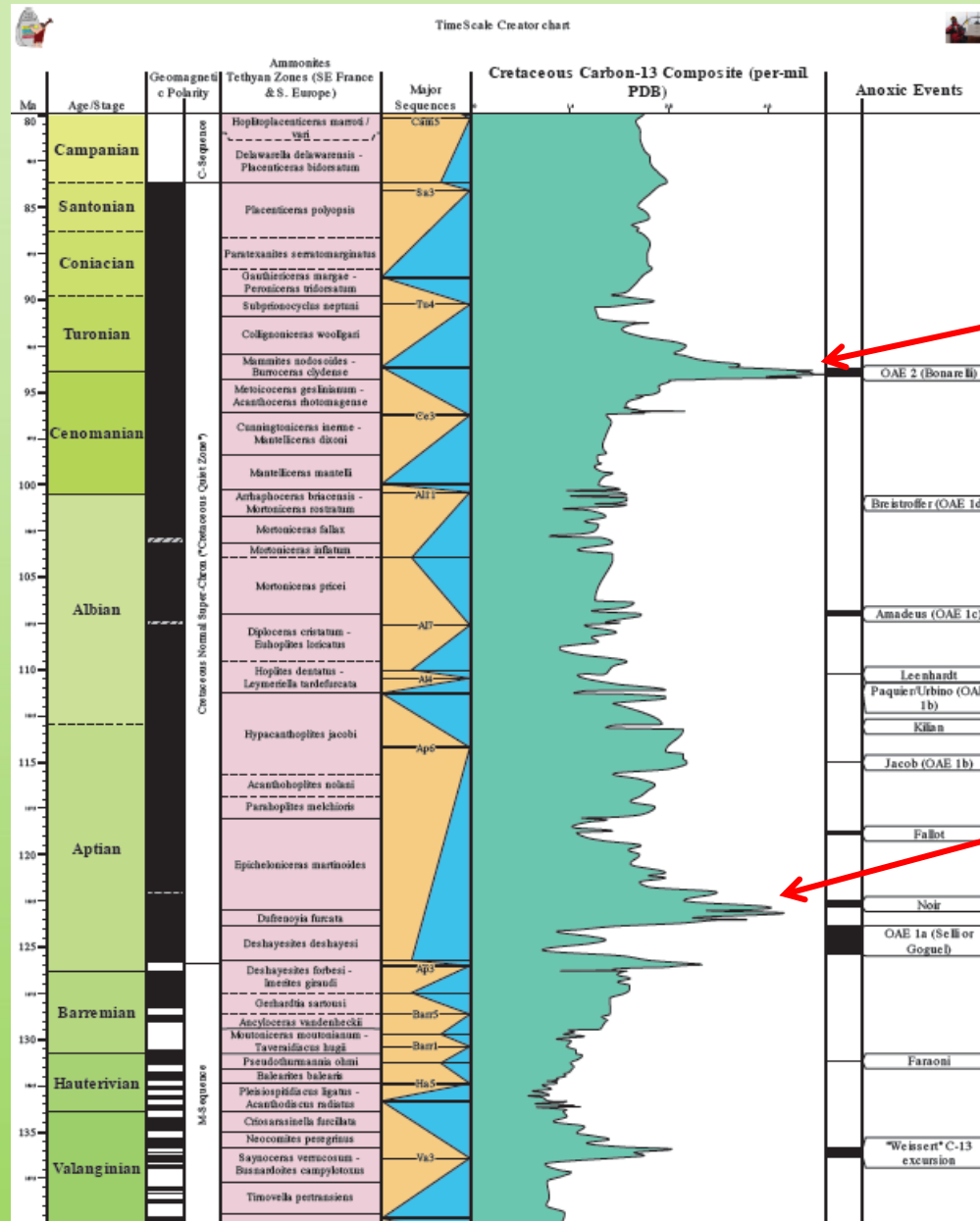
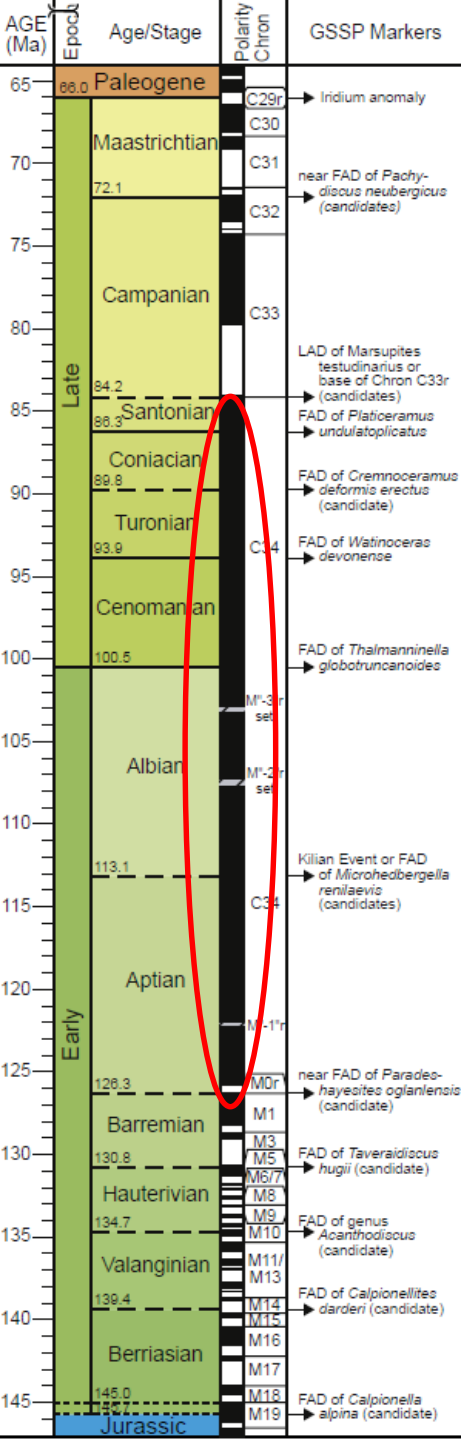
Biota prefer the lighter Carbon (^{12}C) isotope

Burial of marine organic matter ($< ^{12}\text{C}$ in ocean) causes rise in $\delta^{13}\text{C}_{\text{org}}$

**Massive release of methane hydrates causes fall in $\delta^{13}\text{C}_{\text{org}}$
(e.g. PETM)**

Large volcanic episodes ($> ^{12}\text{C}$ in ocean) cause fall in $\delta^{13}\text{C}_{\text{org}}$

Mid-Cretaceous Geomagnetic Quiet Zone complicates GTS, but carbon isotope trends provide global marine/non-marine correlations



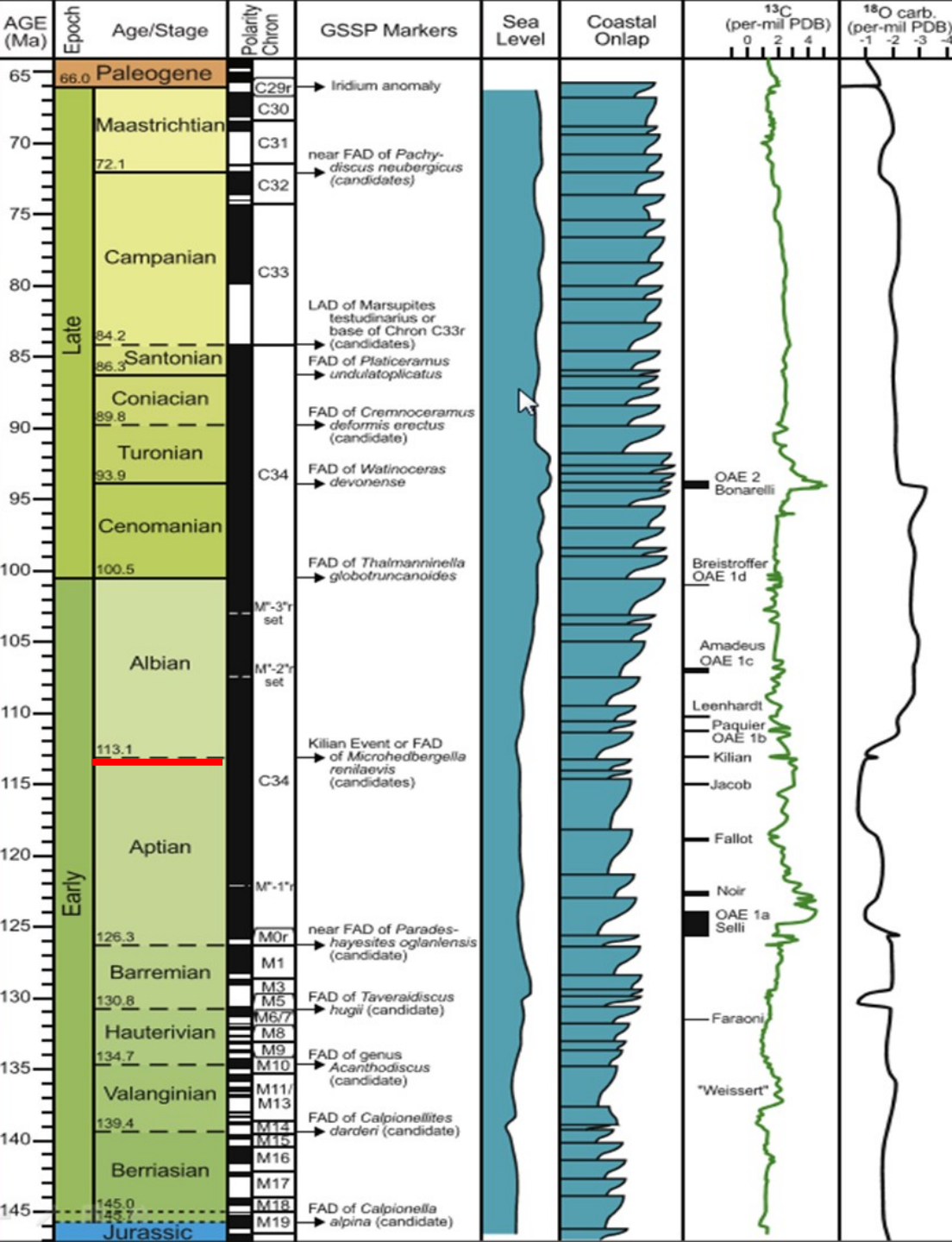
OAE2

OAE1a

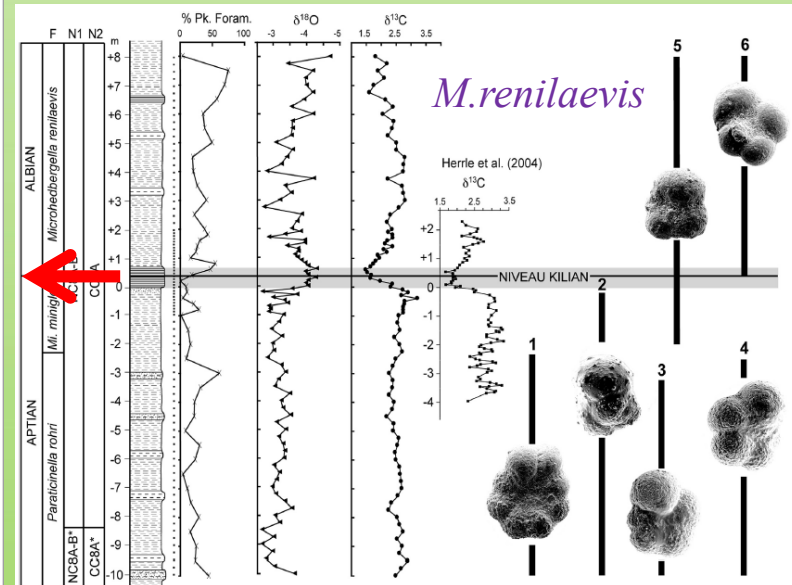
OAE 2 (Bonarelli Event): Cenomanian–Turonian boundary Carbon isotope excursion spans the *M. geslinianum* to *W. devonense* ammonite zones, with the peak in uppermost Cenomanian. The associated organic-rich levels are named Bonarelli in central Italy.



Hesselthal, Germany



Albian GSSP



Also nannofossil, ammonite and carbon isotope proxy markers !

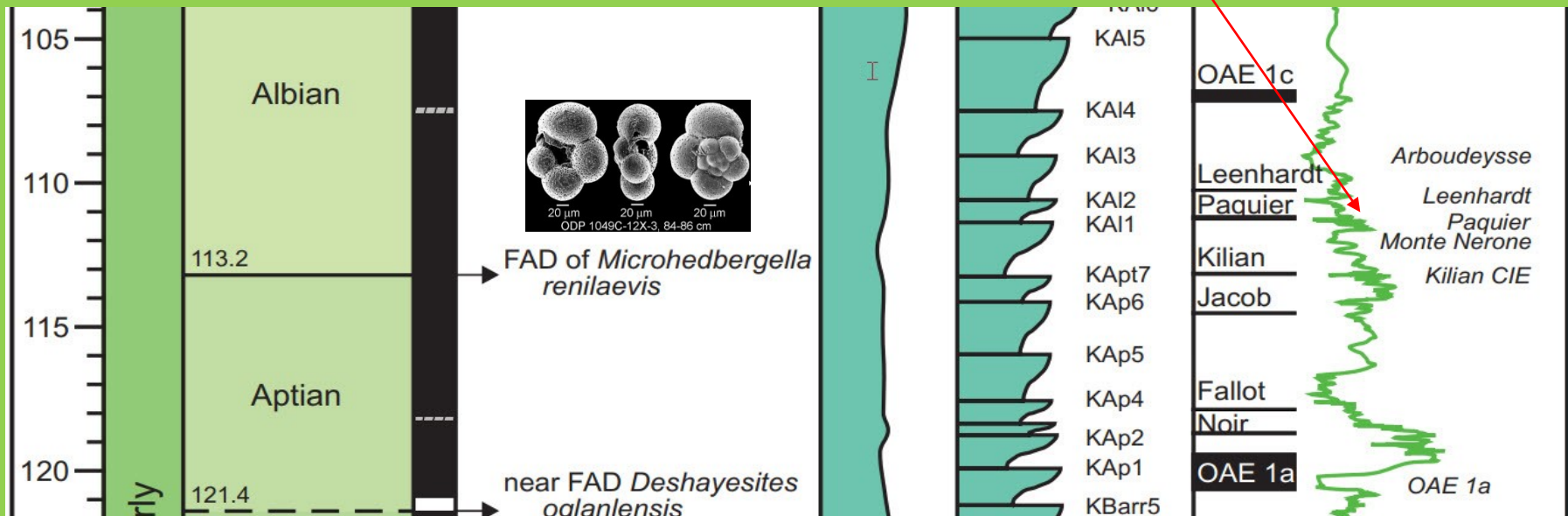
Base Albian GSSP with proxy markers

Lowest occurrence of circular nannofossil *Prediscosphaera columnata* and lowest occurrence of nannofossil *Helicolithus trabeculatus*

Boundary marker: First occurrence of planktonic foraminifer *Microhedbergella renilaevis*.

Lowest occurrence of ammonite *Leymeriella (L) tardefurcata* at base of Niveau Paquier,

Distinctive negative carbon-isotope excursion just above base of Niveau Paquier in the Vocontian Basin, is a local manifestation of Oceanic Anoxic Event 1b.



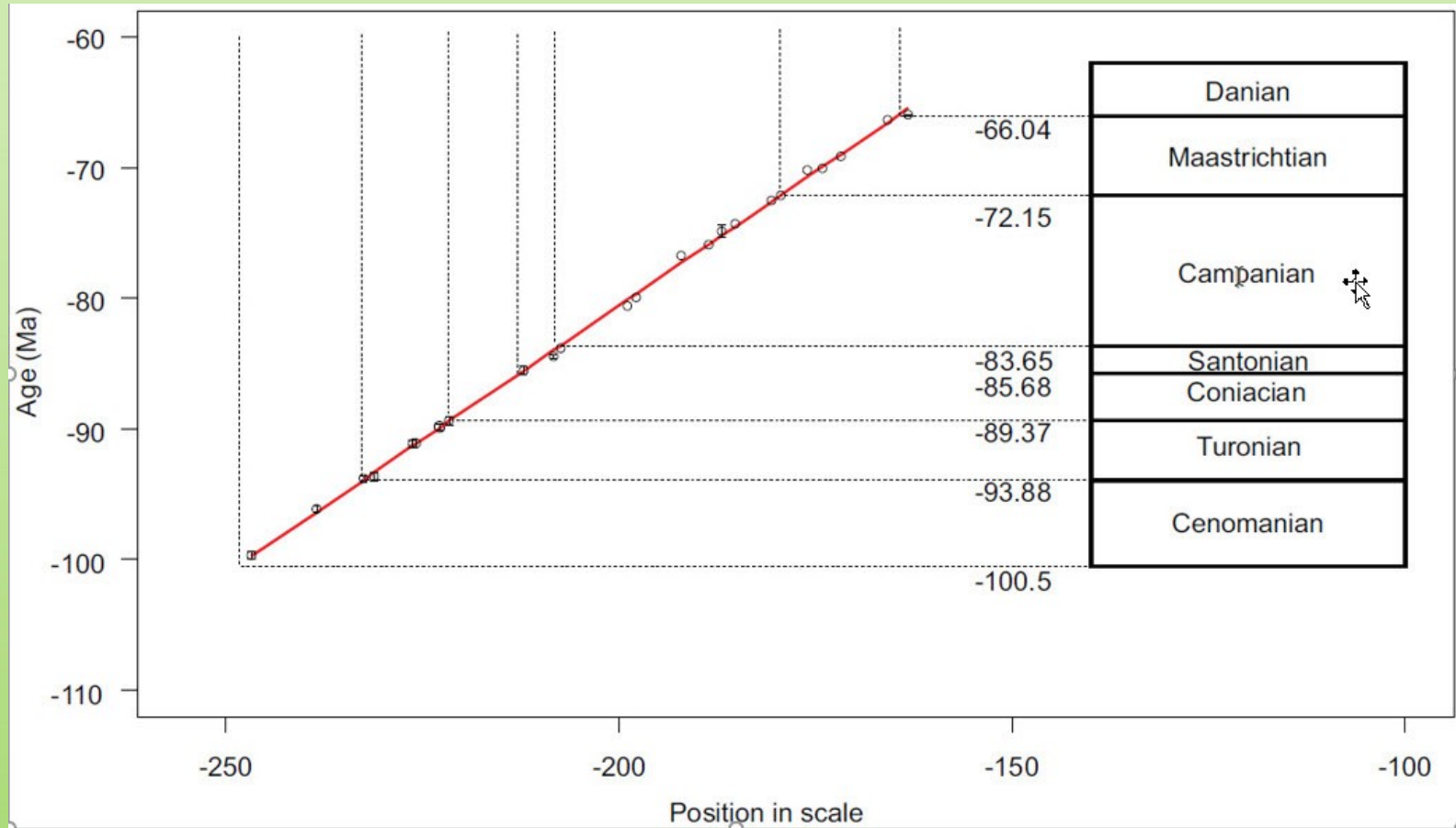
Pres-Guittard, Drôme, France : APTIAN-ALBIAN boundary



Stratigraphic input data for the Late Cretaceous spline

Stage (base)	radiometric age, 2 sigma	name of UK bentonite	cycle and cycle-age assignment	stratigraphy-C chron assignment	mid km C-sequence	Reference
Danian	66.04 ± 0.05					This chapter
			66.31 ± 0.5	top of 30N	1371.84	Batenberg et al. 2012
			69.19 ± 0.5	top of 31N	1409.56	Batenberg et al. 2012
			70.08 ± 0.5	<i>B. clinolobatus</i> Zone ;mid 31R		
			70.65 ± 0.5	top of 32N	1481.12	Batenberg et al. 2012; GTS2012
Maastrichtian			72.5 ± 0.5	<i>B. eliasi</i> Zone; mid 32N		This chapter; Appendix 2
	74.85 ± 0.43		184.5 74.3 ± 0.5	<i>E. jenneyi</i> Zone; top 33N	1549.41	This chapter; Appendix 2
			75.92 ± 0.5	<i>R. calcarata</i> Zone; upper 33N		This chapter; Appendix 2
			76.62 ± 0.5	<i>B. scotti</i> Zone; mid 33N		This chapter; Appendix 2
			197 79.9 ± 0.5	base 33N	1732.76	This chapter; Appendix 2
			~197 80.63 ± 0.5	<i>B. obtusus</i> Zone; beneath base 33N	1723.76	This chapter; Appendix 2
Campanian	83.27 ± 0.11		~ 207	<i>S. leeii III</i> Zone; base 33R	1862.32	S1019 in Wang et al. (2016)
	84.13 ± 0.15			<i>D. bassleri</i> Zone		Sageman et al. (2014)
			207.5	34N		
Santonian	85.59 ± 0.35		86.06 ± 0.35	top <i>C. undulatoaplicatus</i> Zone		This chapter; Appendix 2
Coniacian	89.86 ± 0.26	Lewes Marl	222			Gale 2019
	89.37 ± 0.37	Caburn Marl	224			"
	91.07 ± 0.28	Southerham Marls	225			"
	91.15 ± 0.26	Glynde Marls	226			"
	93.67 ± 0.31	Lutworth Marl	229			"
Turonian	93.79 ± 0.26	C-T bentonite	232 93.65 ± 0.5			Batenberg et al. 2016
mid Cenomanian	96.12 ± 0.31	Thatcher Bentonite	238 96.5 ± 0.5			Batenberg et al. 2016
	99.7 ± 0.3			~ one subzone above GSSP		Takashima et al. 2019
Cenomanian	100.5 ± 0.14					GTS2016 and this chapter

Cenomanan - Maastrichtian cubic spline fit and time scale, using 15 radiometric ages, interpolated with 15 405 kyr cycle derived ages and stage durations, all aligned to the mid km M-sequence, with 7 chron-sequence distances.



Frits Agterberg

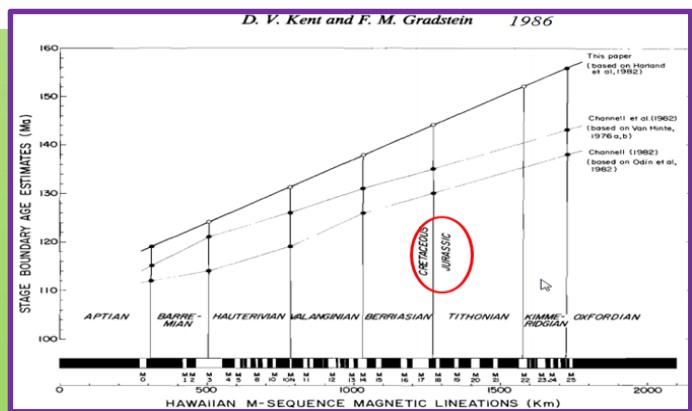
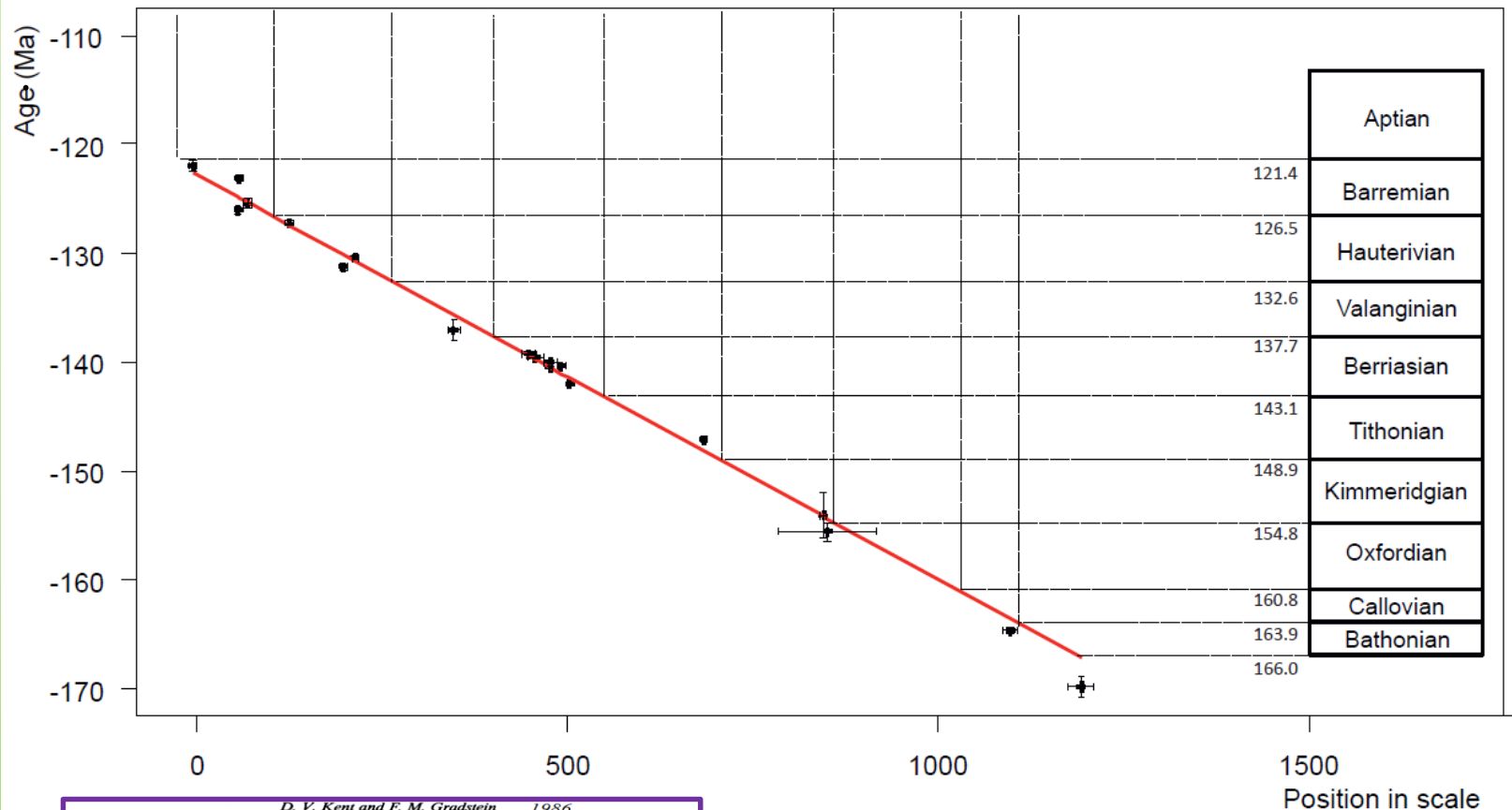
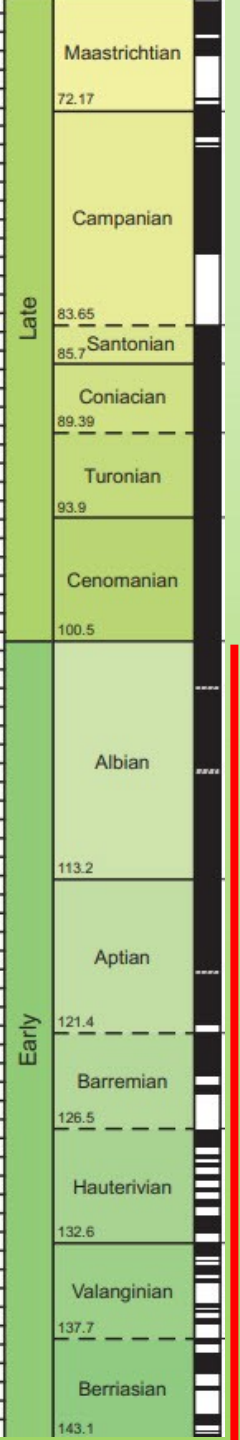
Age of Late Cretaceous stages in GTS2012 and GTS2020

	GTS2012	GTS2020	uncertainty
Maastrichtian	72.1	72.2	0.2
Campanian	83.6	83.7	0.5
Santonian	86.3	85.7	0.2
Coniacian	89.8	89.4	0.2
Turonian	93.9	93.9	0.2
Cenomanian	100.5	100.5	0.1

Stratigraphic input data for the Early Cretaceous spline

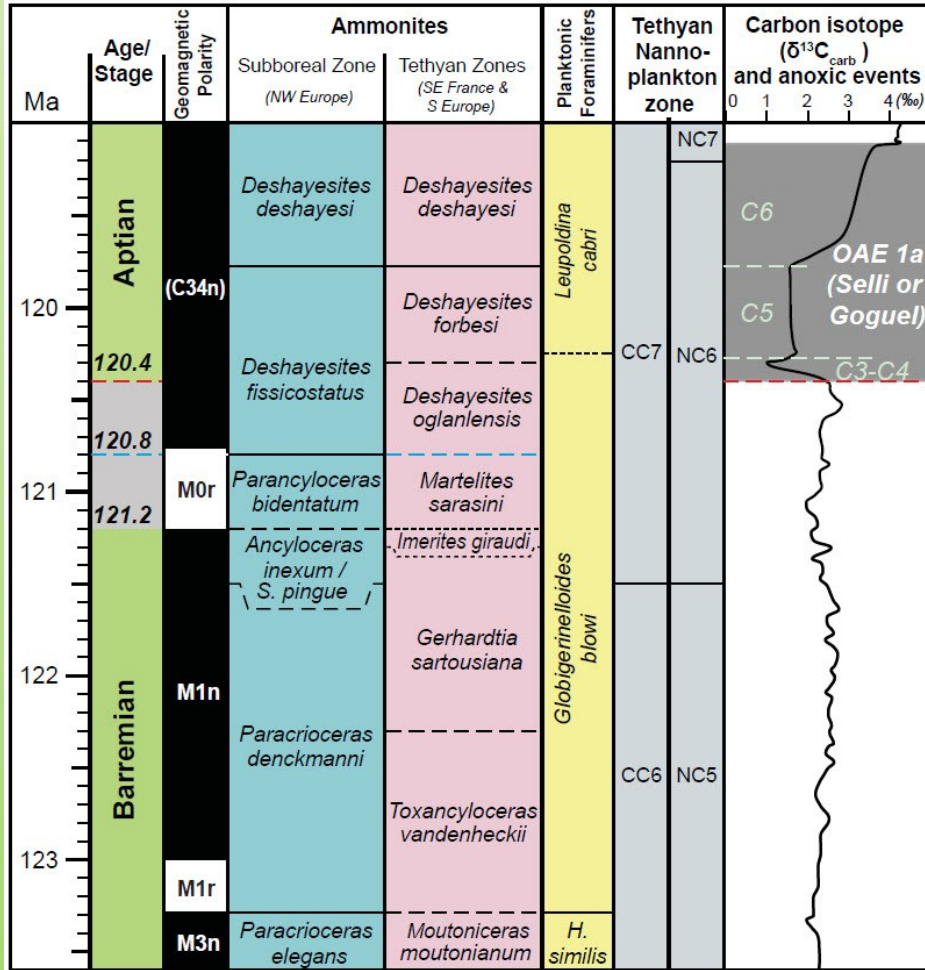
Stage	radiometric age, 2 sigma	interpolated age with cycles	duration from 405 kyr cycles	stratigraphy-chron assignment	mid km M-sequence	Reference
base Cenomanian	100.5 ± 0.14					GTS2016 and this chapter
			Albian duration 12.45 ± 0.5			
base Albian	113.10 ± 0.3					GTS2016 and this chapter
early Aptian	121.20 ± 1			several ages dates in Appendix 2		
near base Aptian	122.01 ± 0.52			no biostrat; whole M0r	minus 4.9 ± 4.9	He et al. 2008; this chapter
			Aptian duration 8.1 ± 0.5			
base Aptian				near chron M0r	0 ± 2.5	
mid Barremian	123.10 ± 0.3			upper half of M1r	55.8 ± 2.2	Zhang et al. 2018 and in press; this chapter
Barremian	125.45 ± 0.43			entire M1r	68.5 ± 6.1	Pringle & Duncan, 1995
			Barremian duration 5.00 ± 0.5			
base Barremian		126.07 ± 0.25		upper part of chron M5n	120 ± 5	
Hauterivian	127.24 ± 0.25 (2σ approx.)			upper Hauterivian, mid M5n	125.5 ± 5.5	Return to Agrio
Hauterivian	130.39 ± 0.25 (2σ approx.)			uppermost M10N	213.5 ± 4.6	Aquirre-Uretta et al. 2017
			Hauterivian duration 5.93 ± 0.5			
base Hauterivian	131.29 ± 0.25			in chron M10n	198 ± 4	Aquirre-Urreta et al. in press
			Valanginian duration 5.06 ± 0.5			
base Valanginian		137.05 ± 1.0		chron M14r.3	347 ± 9	Martinez et al. 2015
Berriasian	139.24 ± 0.16			uppermost M17r	447.8 ± 9.9	Lena et al. 2019
	139.55 ± 0.18			M17r	457.7 ± 9.9	Vennari et al., 2014
	139.96 ± 0.17			M18n-M17r boundary interval	476.9 ± 9.3	Lena et al. 2019
	140.34 ± 0.18			M18r - M18n boundary interval	491.8 ± 5.8	„ „
	140.51 ± 0.16			base M18n to lower M17r	476.3 ± 19.6	„ „, revised Ogg, pers. comm.
	142.04 ± 0.17			lower M18r	503 ± 2.1	„ „
	146.48 ± 1.63			M18r - M18n boundary interval	500 ± 5.1	Mahony et al. 2005
			Berriasian duration 5.27 ± 0.5			Kietzmann et al. 2018
base Berriasian				mid M19n.2n	526.3 ± 14	Berriasian Working Group, ICS
Tithonian	147.11 ± 0.18			early Tithonian; upper M22r	684.7 ± 4.3	Lena et al. 2019
			Tithonian duration 5.67 ± 0.5			Kietzmann et al. 2018
base Tithonian				base chron M22An	701 ± 2	

Early Cretaceous – Middle Jurassic cubic spline fit and time scale, using 25 radiometric ages, interpolated with ten 405 kyr cycle derived ages and stage durations, all aligned to the mid km M-sequence with 18 chron-sequence distances



Frits Agterberg

Short Aptian in GTS2020



Age estimates using three definition for base Aptian

Long Aptian (13.3 myr) in GTS2012 with base at 126.3 Ma

Duration of Aptian Stage based on high-resolution cyclostratigraphic interpretation of the Piobboco core of central Italy (Huang et al., 2010) relative to a U-Pb date of 113.1 ± 0.3 Ma near the Aptian/Albian boundary (see Ogg et al., 2012).

Short Aptian (8.2 myr) in GTS2020 with base at 121.3 Ma

Piobboco core Milankowich cyclicity is wrong.

Hauterivian-Barremian boundary at 126.02 Ma (Martinez et al., 2015).

Magnetostratigraphy of U-Pb-dated boreholes in Svalbard, Norway, implies that magnetochron M0r begins at 121.2 ± 0.4 Ma (Zhang et al., 2019)

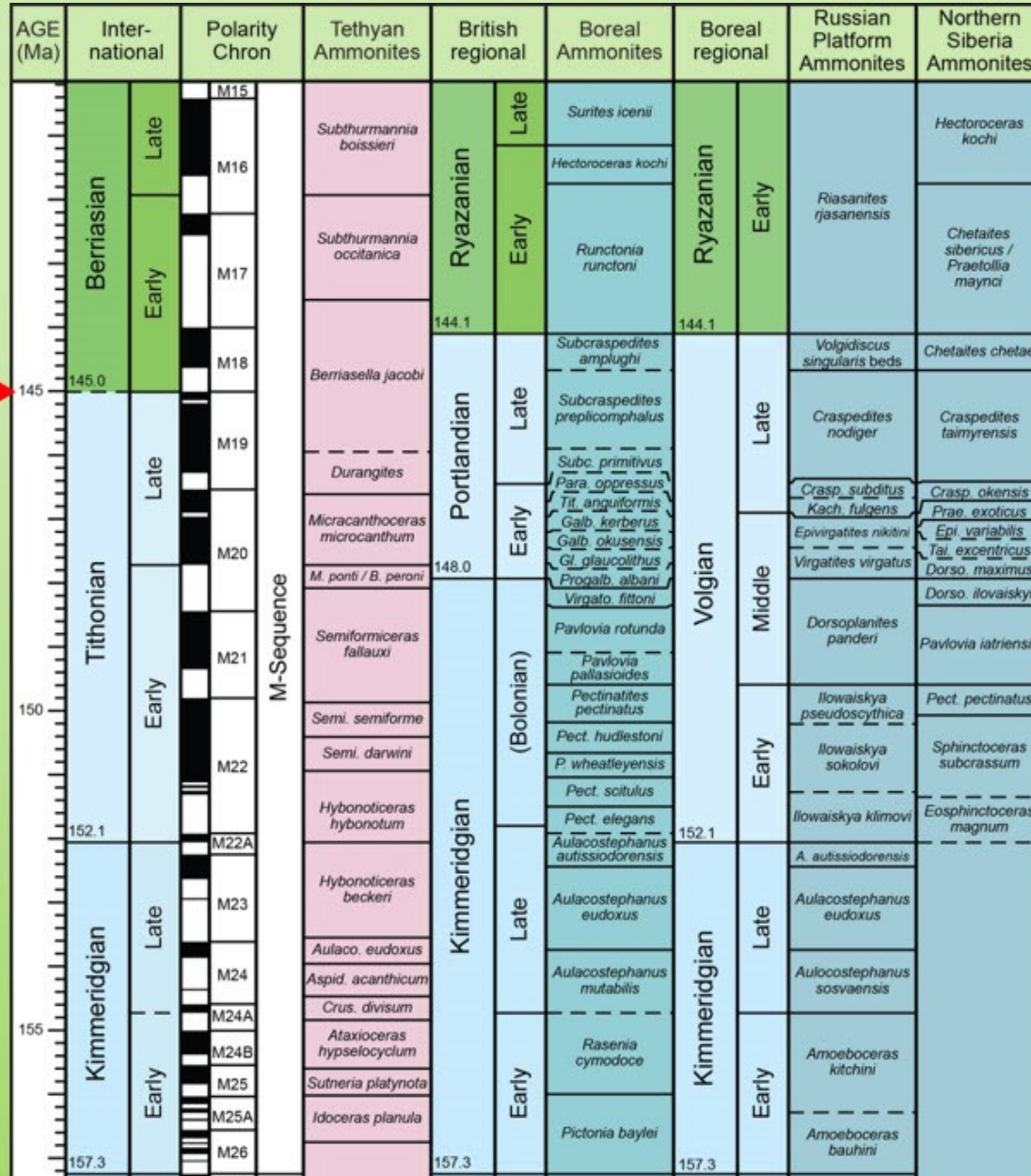
Spreading rate estimates change the date of the base Aptian to 121.5 Ma (Malinverno et al., 2012).

Berriasian through Aptian stage ages and stage durations

	GTS2012	GTS2020	s.d.
Albian	113.0	113.2	0.3
Aptian	126.3	121.4	0.6
Barremian	130.8	126.5	0.7
Hauterivian	133.9	132.6	0.6
Valanginian	140.2	137.7	0.5
Berriasian	145.0	143.1	0.6

	GTS2012	GTS2020
Aptian	13.3	8.2
Barremian	4.5	5.1
Hauterivian	3.8	6.1
Valanginian	5.5	5.1
Berriasian	5.6	5.4

Endless Jurassic-Cretaceous boundary deliberations (No boundary definition !)



Nothing really happens at the J/K boundary !

First order eustatic sealevel is relatively low.

There is severe fossil endemism, leading to local stages and great confusion in correlation.

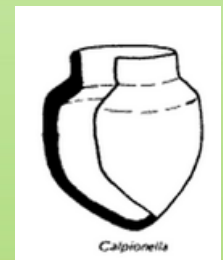
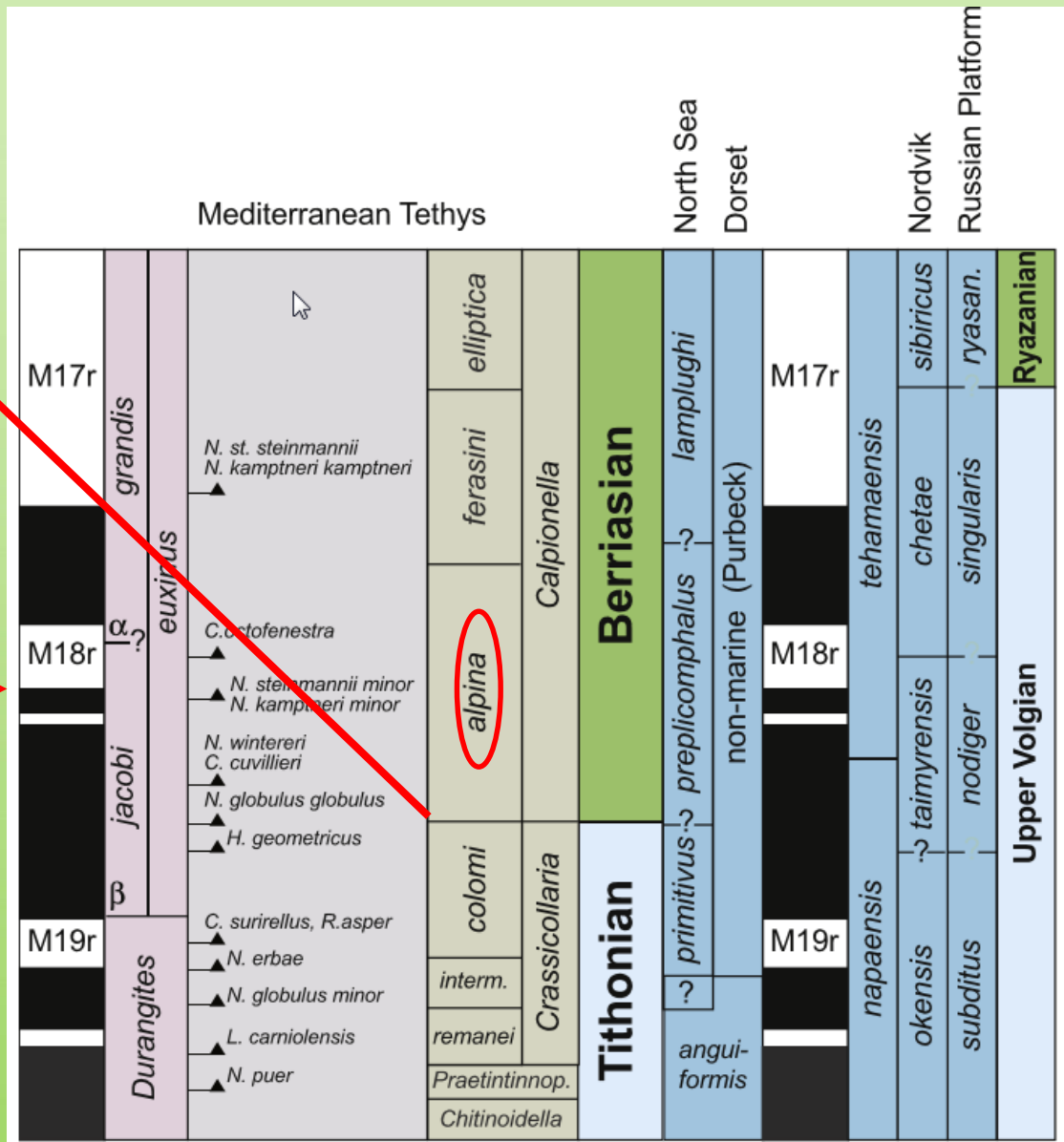
MFIBTYF
and geomag or stable isotopes cannot be seen in outcrops....

New Definition for the Jurassic-Cretaceous boundary

the only Period boundary without a ratified definition

Cenozoic	Neogene	Pliocene
	Paleogene	Oligocene
		Eocene
		Paleocene
	Mesozoic	Cretaceous
Early		
Jurassic		Late
		Middle
		Early
Triassic	Late	
	Middle	
	Early	
Permian	Lopingian	
	Guadalupian	
	Cisuralian	
Paleozoic	Carboniferous	Pennsylvanian
		Mississippian
	Devonian	Late
		Middle
		Early
Silurian	Pragian	
	Llandovery	
Ordovician	Late	
	Middle	
	Early	
Cambrian	Furongian	
	Early	

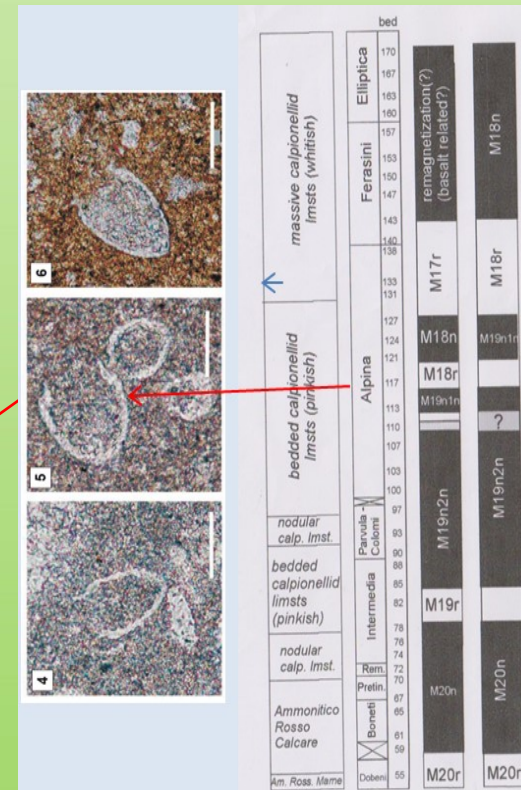
Old →



Tethyan Ammonites
 Calc. Nannoplankton
 α 1965 colloquium decision on J/K boundary
 Boreal Ammonites
 Calpionellids
 β 1975 colloquium decision on J/K boundary

Ammonitico Rosso type limestones across the J/Cr boundary Veliky Kamenets, W. Ukraine

Nothing really happens at the J/K boundary !





Las dos tetas

Cretaceous 'hothouse'